



HAL
open science

Robust Two-Coordinate Zn(II) Organocations Supported by Bulky-Yet-Flexible IPr* Carbene: Synthesis, Structure, and Distinct Reactivity in Hydrosilylation Catalysis

Xuejuan Xu, Christophe Gourlaouen, Béatrice Jacques, Samuel Dagorne

► **To cite this version:**

Xuejuan Xu, Christophe Gourlaouen, Béatrice Jacques, Samuel Dagorne. Robust Two-Coordinate Zn(II) Organocations Supported by Bulky-Yet-Flexible IPr* Carbene: Synthesis, Structure, and Distinct Reactivity in Hydrosilylation Catalysis. *Organometallics*, 2023, 42 (19), pp.2813-2825. 10.1021/acs.organomet.3c00282 . hal-04295782

HAL Id: hal-04295782

<https://hal.science/hal-04295782>

Submitted on 24 Nov 2023

HAL is a multi-disciplinary open access archive for the deposit and dissemination of scientific research documents, whether they are published or not. The documents may come from teaching and research institutions in France or abroad, or from public or private research centers.

L'archive ouverte pluridisciplinaire **HAL**, est destinée au dépôt et à la diffusion de documents scientifiques de niveau recherche, publiés ou non, émanant des établissements d'enseignement et de recherche français ou étrangers, des laboratoires publics ou privés.

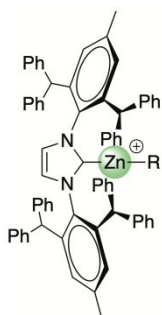
Robust two-coordinate Zn(II) organocations supported by bulky-yet-flexible IPr* carbene: synthesis, structure and distinct reactivity in hydrosilylation catalysis

Xuejuan Xu, Christophe Gourlaouen, Béatrice Jacques and Samuel Dagorne*

*Institut de Chimie (UMR CNRS 7177), CNRS - Université de Strasbourg, 4, rue Blaise Pascal
67000 Strasbourg, France*

Email : dagorne@unistra.fr

For TOC Use Only



- Improved hydrolytic stability thanks to NHC steric and electronic stabilization
- Effective hydrosilylation catalysts of alkynes and carbonyls

Abstract. The present study details the synthesis and characterization of novel Zn(II)-based organocations of the type $[\text{IPr}^*-\text{Zn}-\text{R}]^+$ ($\text{IPr}^* = 1,3\text{-bis}[2,6\text{-bis}(\text{diphenylmethyl})\text{-4-methylphenyl}]\text{-}1,3\text{-dihydro-}2H\text{-imidazol-}2\text{-ylidene}$; $\text{R} = \text{alkyl, aryl}$) and their use in styrene, alkyne and carbonyls hydrosilylation catalysis. The neutral IPr^* adducts $[\text{IPr}^*-\text{ZnR}_2]$ (**1**, $\text{R} = \text{Me}$; **2**, $\text{R} = \text{Et}$; **3**, $\text{R} = \text{Ph}$) were prepared by reaction of IPr^* with an equimolar amount of ZnR_2 and isolated in good yields. Despite the severe steric hindrance of IPr^* , compounds **1-3** are robust in solution, reflecting the *bulky-yet-flexible* nature of carbene IPr^* . Adducts **1** and **2** can be readily ionized by $[\text{Ph}_3\text{C}][\text{B}(\text{C}_6\text{F}_5)_4]$ to produce two-coordinate Zn(II) cations $[\text{IPr}^*-\text{ZnMe}]^+$ (**[4]⁺**) and $[\text{IPr}^*-\text{ZnEt}]^+$ (**[5]⁺**), both isolated in high yields ($> 85\%$) as $[\text{B}(\text{C}_6\text{F}_5)_4]^-$ salts. Interestingly, the more Lewis acidic cation $[\text{IPr}^*-\text{ZnC}_6\text{F}_5]^+$ (**[6]⁺**), prepared by reaction of **[4]** $[\text{B}(\text{C}_6\text{F}_5)_4]$ with a $\text{B}(\text{C}_6\text{F}_5)_3/\text{HSiEt}_3$ mixture, is further stabilized through π arene interactions with the Zn(II), indicating that IPr^* may provide steric *and* electronic stabilization to Zn(II). The latter certainly explains the improved hydrolytic stability of salt **[6]** $[\text{B}(\text{C}_6\text{F}_5)_4]$. Zn cations of the $[\text{IPr}^*-\text{ZnR}]^+$ series are less Lewis acidic than their $[\text{IPr}-\text{ZnR}]^+$, yet displaying a distinct reactivity in hydrosilylation catalysis. Thus, cation **[6]⁺** catalyzes at room temperature styrene and alkyne hydrosilylation with HSiEt_3 as a silane source. Remarkably, it is also a highly effective ketone/aldehyde hydrosilylation catalysis for a rather broad silane and ketone scope, and perform much better than $[\text{IPr}-\text{ZnR}]^+$ systems. The DFT-estimated mechanism for hydrosilylation benzophenone by **[6]⁺** suggests that Si-H activation by the cationic Zn(II) center is required for the catalysis to proceed. Overall, the **improved hydrolytic** stability and straightforward synthesis of a well-defined Zn-based Lewis acid such as **[6]** $[\text{B}(\text{C}_6\text{F}_5)_4]$ may promote its further use in various Lewis-acid-mediated transformations.

Introduction

Thanks to their steric tunability and exceptional σ -donating properties, N -heterocyclic carbenes (NHCs) constitute a privileged class of supporting ligands for the stabilization of various metal/heteroatom centers, leading to widespread applications across chemical science over the past 25 years.^{1,2,3,4,5} Most notably, the ability of NHC ligands to stabilize reactive organometallics through coordination to various metal/heteroatom centers has led to significant achievements in metal-mediated homogeneous catalysis and fundamental reactivity of organometallics.^{6,7,8,9,10,11} First reported by Markó and co-workers,¹² highly sterically bulky NHCs such as IPr* (Figure 1) and related have recently attracted interest for coordination to several metal centers because of their *bulky-yet-flexible* nature: *i.e.* a severe steric bulk for protection/stabilization of the metal center combined with flexibility of the bulky N -substituents allowing substrate approach if need be.^{13,14,15} Notably, Pd(II), Cu(I), Au(I), Ru(II) and Pt complexes of such ligands, which have been most studied,^{16,17,18,19,20,21,22,23,24,25,26} were shown to exhibit superior catalytic performances and/or enhanced stability (*versus* more classical NHCs) on a number of occasions due to IPr* steric protection to the catalytically active species. In contrast, despite their attractive features, the coordination of IPr*-type ligands with oxophilic, high-oxidation-state and Lewis acidic metal centers is unexplored with the exception of couple of IPr* adducts of Ga(III)/In(III), found to exhibit significantly improved stability versus analogous NHC-Ga/In adducts.²⁷

NHC-stabilized Zn(II) species have attracted a growing attention over the past few years because the enhanced stability provided NHC ligation to Zn(II) may lead to novel/robust organozinc species for use in catalytic applications, the use of a cheap and non-toxic metal source such as Zn being particularly attractive.^{28,29} NHC-Zn compounds have thus far been used for the catalysis of a variety of transformations ranging from hydrosilylation of unsaturated substrates (primarily alkenes, alkynes, nitriles and CO₂), allylic alkylation, alkyne

dehydroboration/diboration, alkyne hydroboration, C-H borylation of heteroarenes to polymerization catalysis of polar monomers.^{28,29,30,31,32,33} In the area, we earlier showed that, thanks to NHC stabilization, two-coordinate **organozinc cations** of the type $[\text{IPr-Zn-R}]^+$ (R = alkyl, aryl) are viable and isolable species despite their strong electrophilicity and Lewis acidity: such electrophiles were found to be effective catalysts for CO_2 , alkene and alkyne hydrosilylation as well as alkyne hydroboration.^{34,32} However, the poor hydrolytic stability and substrates tolerance of $[\text{IPr-Zn-R}]^+$ cations prompted us towards the use of *bulky-yet-flexible* NHC such as IPr* to access two-coordinate $[\text{IPr}^*\text{-Zn-R}]^+$ cation **with improved hydrolytic stability**, yet possibly retaining enough reactivity for substrates activation. In addition to steric protection, a ligand such as IPr* may also provide additional electronic stabilization to electrophilic Zn^{II} cations through arene π -stabilization (with the N- CHPh_2 groups of the NHC ligand). As recently observed, low-coordinate **organozinc cations** may form labile M-arene complexes.^{35,36,37}

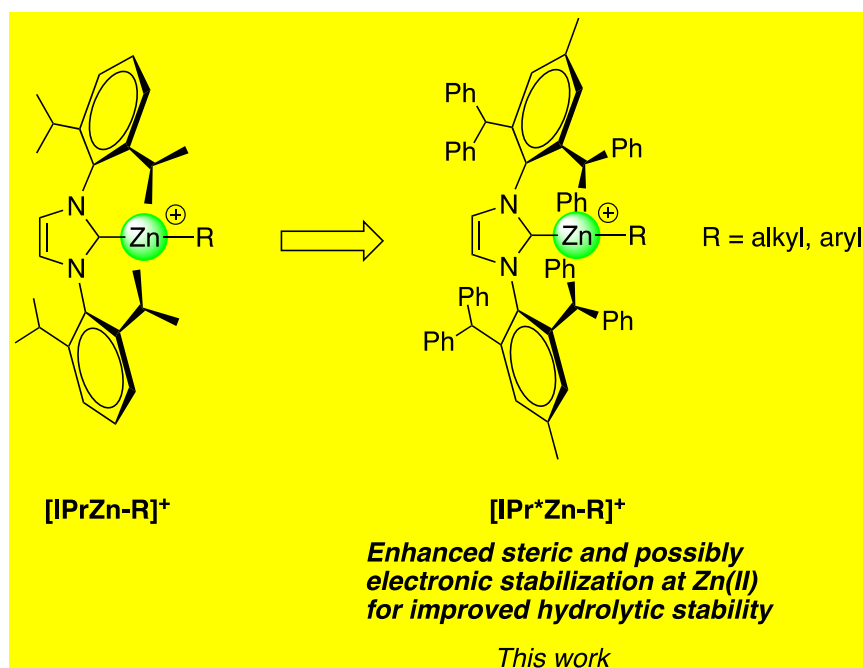


Figure 1. Studied organozinc cations $[\text{IPr}^*\text{Zn-R}]^+$

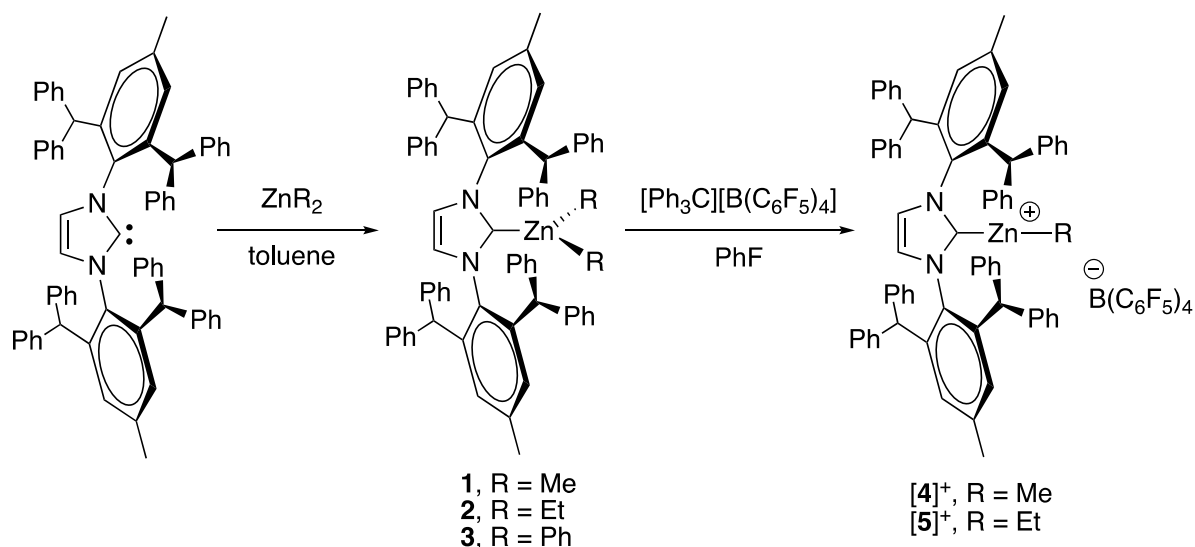
We herein report on the synthesis and structure of $[\text{IPr}^*\text{-Zn-R}]^+$ organocations (R = alkyl, aryl; Figure 1) and their use as catalysts in styrene, ketones, aldehydes and CO_2 hydrosilylation. As shown below, besides improved stability, such cations were found in some instances to perform better than benchmark $[\text{IPr-Zn-R}]^+$ catalysts also tested for comparison. DFT calculations were also performed to support experimental results and provide mechanistic understanding of ketone hydrosilylation catalysis.

Results – Discussion

Synthesis and structure of the NHC-supported Zn(II) complexes **1-3** and **[4-6][B(C₆F₅)₄]**.

Access to $[\text{IPr}^*\text{-Zn-R}]^+$ organocations was carried out through ionization of the corresponding neutral precursors $[\text{IPr}^*\text{-ZnR}_2]$ (R = Me, Et, Ph; **1-3**, Scheme 1), thus requiring the initial preparation of adducts **1-3**. The latter were readily accessed by reaction of carbene IPr^* , prepared according to a literature procedure,¹⁹ with 1 equiv of ZnR_2 (R = Me, Et, Ph; toluene, 2 h) to quantitatively afford adducts **1-3**, all isolated in high yields as analytically pure colorless powders. In solution, NMR data support adducts formation with, in particular, a characteristic upfield chemical shift of the $\text{C}_{\text{carbene}}$ signal in **1-3** (ranging from 185 to 188 ppm versus 220.0 ppm for free IPr^*), indicating effective NHC coordination to the Zn(II) center despite the greater steric hindrance imposed IPr^* .³⁸ The solid state molecular structures of adducts **1** and **3** were established through X-ray crystallographic analysis (see Supporting Information for further details), and are depicted in Figures 2 and 3. Both complexes contain a central NHC-stabilized and three-coordinate Zn(II) center with Zn-NHC bond distances (2.112(3) and 2.089(1) Å in species **1** and **3**, respectively) nearly identical to that in $[\text{IPr-ZnMe}_2]$ (2.112(2) Å), reflecting that the *bulky-yet-flexible* nature of IPr^* .³⁸ Thus, in adducts **1** and **3**, all Ph groups of the N-R substituents of the IPr^* ligand point away from the ZnR_2 moiety so that to minimize steric repulsions (Figures 2 and 3). Also in line with robust $[\text{IPr}^*\text{-ZnR}_2]$ adducts, DFT-estimated

binding energies (wB97XD/6-31+G** theory level) between IPr*/IPr and ZnMe_2 were done for comparison, and suggest that adduct $[\text{IPr}^*\text{-ZnMe}_2]$ ($\text{DG} = -6.4 \text{ kcal.mol}^{-1}$) is even more stable than $[\text{IPr}\text{-ZnMe}_2]$ ($\text{DG} = -2.1 \text{ kcal.mol}^{-1}$), which is probably due to stronger London dispersion interactions in $[\text{IPr}^*\text{-ZnMe}_2]$.



Scheme 1. Synthesis of IPr* adducts [1-3] and derived Zn-alkyl organocations

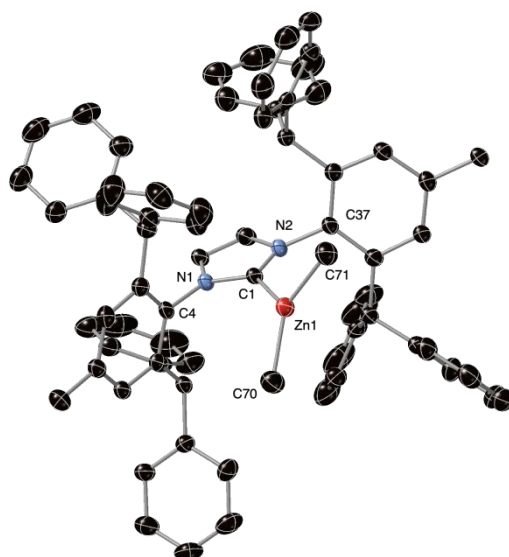


Figure 2. Molecular structure (ORTEP view) of neutral adduct $[\text{IPr}^*\text{-ZnMe}_2]$ (**1**). Selected bond distances (\AA) and angles ($^\circ$). $\text{Zn1-C1} = 2.112(3)$, $\text{C1-N1} = 1.364(4)$, $\text{C1-N2} = 1.359(5)$, $\text{Zn1-C70} = 1.985(4)$, $\text{Zn1-C71} = 1.994(4)$, $\text{C70-Zn1-C71} = 134.02(18)$, $\text{C70-Zn1-C1} = 115.61(16)$, $\text{C71-Zn1-C1} = 110.10(15)$.

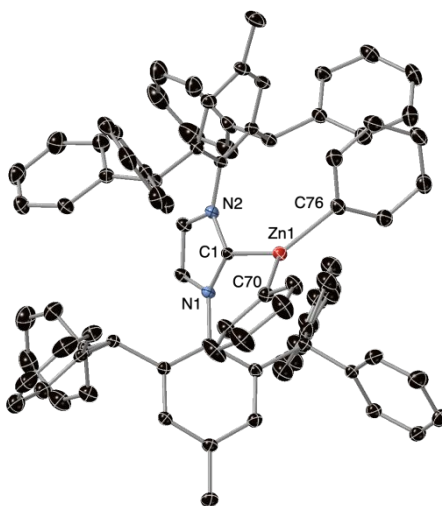


Figure 3. Molecular structure (ORTEP view) of neutral adduct [IPr*-ZnPh₂] (**3**). Selected bond distances (Å) and angles (°). Zn1-C1 = 2.089(1), C1-N1 = 1.360(2), C1-N2 = 1.362(2), Zn1-C70 = 1.981(1), Zn1-C76 = 2.001(1), C70-Zn1-C76 = 125.62(6), C70-Zn1-C1 = 118.6(6), C76-Zn1-C1 = 115.52(6).

The Zn-alkyl organocations [IPr*-ZnR]⁺ (**[4]**⁺, R = Me; **[5]**⁺, R = Et; Scheme 1) were readily accessed *via* **alkyl** abstraction of the corresponding neutral precursors **1** and **2**, respectively. Thus, reaction of **1-2** with 1 equiv of [Ph₃C][B(C₆F₅)₄] (PhF, 2 h, RT) quantitatively yielded the corresponding [IPr*-ZnR]⁺ (R = Me, Et; **[4]**⁺ and **[5]**⁺), which were isolated in a pure form as [B(C₆F₅)₄]⁻ salts in 85% and 87% yields, respectively. In contrast, ionization of adduct [IPr*-ZnPh₂] (**3**) with 1 equiv of [Ph₃C][B(C₆F₅)₄] led to an intractable mixture of unknown products on the basis of ¹H NMR data, indicating that Zn-Ph abstraction by [Ph₃C][B(C₆F₅)₄] may not readily and cleanly occur at NHC-ZnPh₂ systems. Salts **[4-5]**[B(C₆F₅)₄]⁻ are stable for weeks in CD₂Cl₂ under inert atmosphere. NMR data for cations **[4]**⁺ and **[5]**⁺ are all consistent with the formation of [IPr*-ZnR]⁺ cations. In particular, taking the example of **[4]**⁺, the C_{carbene} ¹³C NMR resonance (d = 165.3 ppm) is significantly upfield shifted compared to that of neutral precursor **1** (d = 185.5 ppm), in line, as expected, with a much more Lewis acidic Zn(II) center in **[4]**⁺.³⁹ Salts **[4-5]**[B(C₆F₅)₄]⁻ were also analyzed by 2D ¹H and ¹⁹F DOSY NMR to evaluate cation/anion interactions in solution. In CD₂Cl₂ (RT), the 2D ¹H and ¹⁹F DOSY NMR data for

[4][B(C₆F₅)₄] lead to estimated hydrodynamic radii of 1834 Å and 939 Å (see Supporting Information). The difference between those two values and the fact that the estimated volume for the [B(C₆F₅)₄]⁻ anion is around 900 Å (from solid state data) strongly suggest fully dissociated [IPr^{*}-ZnMe]⁺ and [B(C₆F₅)₄]⁻ ions in CD₂Cl₂. Similar hydrodynamic volumes (2234 Å and 1070 Å from ¹H and ¹⁹F DOSY NMR data, respectively) were also estimated for [5][B(C₆F₅)₄], indicating dissociated ions in CD₂Cl₂. However, DOSY NMR data for [5][B(C₆F₅)₄] recorded in C₆D₅Br, a less polar and dissociative solvent, are consistent with the presence of [5]⁺/[B(C₆F₅)₄]⁻ contact ions pairing to some extent, likely in equilibrium with fully dissociated ions (estimated hydrodynamic volumes from ¹H and ¹⁹F DOSY NMR in C₆D₅Br: 2554 Å and 2054 Å, respectively).

In the solid state, as established through XRD studies, salt [5][B(C₆F₅)₄] crystallizes as discrete and fully dissociated [IPr^{*}-ZnEt]⁺ and [B(C₆F₅)₄]⁻ ions (Figure 4). The cation displays a central *sp*-hybridized and two-coordinate Zn(II) center with Zn–C_{carbene} and Zn–alkyl bond distances (1.968(3) and 1.944(4) Å, respectively), similar to those in cation [IPr-ZnMe]⁺.³⁴ Interestingly, due to the enhanced Lewis acidity of the Zn(II) and the steric relief upon going from a ZnR₂ to Zn–R⁺ moiety (*vs.* neutral precursor [2]), two of the Ph groups of the NHC *N-R* substituents now point towards Zn(II) with short electrostatic contacts (Zn1⋯C25 = 3.071 Å and Zn1⋯C26 = 3.081 Å) close to the sum of van der Waals radii of Zn and C_{sp2} atoms (3.10 Å).⁴⁰

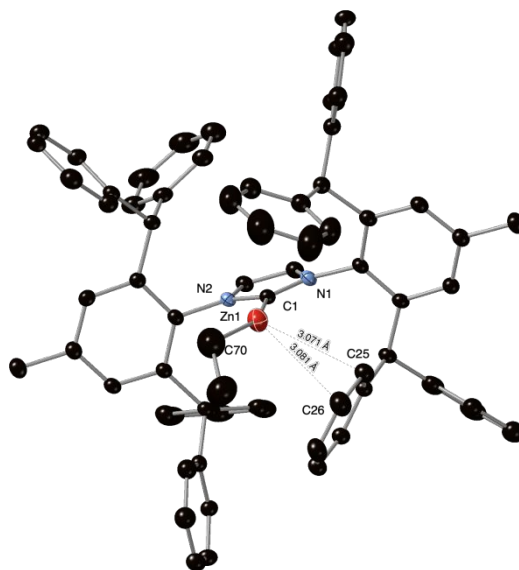
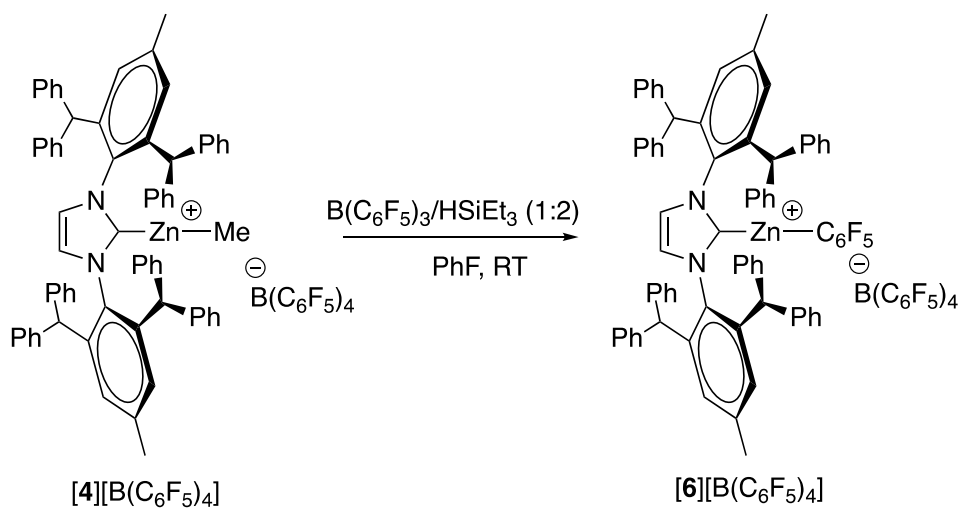


Figure 4. Molecular structure (ORTEP view) of Zn cation [(IPr*)ZnEt]⁺. Selected bond distances (Å) and angles (°). Zn1-C1 = 1.968(3), C1-N1 = 1.346(3), C1-N2 = 1.357(3), Zn1-C70 = 1.944(4), C70-Zn1-C1 = 149.4(2).

Access to the Zn–C₆F₅ cationic derivative [IPr*–ZnC₆F₅]⁺ (**[6]**⁺, Scheme 2), expected to more Lewis acidic than Zn-alkyl cations **[4]**⁺ and **[5]**⁺, was also achieved. Thus, cation [IPr*–ZnMe]⁺ (**[4]**⁺) smoothly reacted with a 1/2 B(C₆F₅)₃/HSiEt₃ mixture (PhF, 24 h, RT) through a Me/C₆F₅ ligand exchange reaction, to quantitatively form **[6][B(C₆F₅)₄]** along with organo-boron/-silicon side-products that were not further studied and characterized. Salt **[6][B(C₆F₅)₄]** was isolated in 84% yield and its molecular structure was established through XRD studies. The latter salt crystallizes as fully dissociated **[6]**⁺ and [B(C₆F₅)₄][–] ions. As shown in Figure 5, cation **[6]**⁺ consists of a two-coordinate Zn(II) cationic center stabilized by a IPr* ligand and a [C₆F₅][–] moiety. While the geometrical/bonding parameters of **[6]**⁺ are for the most part similar to those in the Zn–Et⁺ cation **[4]**⁺, the Zn(II) center in **[6]**⁺, unlike that in **[4]**⁺, is however sandwiched by two Ph rings (of the NHC substituents) with rather short Zn-Ph contacts (Zn1⋯C44 = 2.743 Å, Zn1⋯C49 = 2.862 Å; Figure 5) well below the sum of the corresponding van der Waals radii (3.10 Å),⁴⁰ likely indicative of Zn⋯Ph π -interactions. In line with the latter, DFT-estimated Non Covalent Interactions (NCI) of a model of cation **[6]**⁺, **VI** (Figure 6),

further confirm substantial attractive Van der Waals interactions between the Zn center and the two “sandwiching” Ph rings. These structural and computational data are in line with a more Lewis acidic Zn(II) in **[6]**⁺ vs. cations **[4]**⁺ and **[5]**⁺, as expected when going from Zn-alkyl to Zn-C₆F₅ organocations. In solution, all NMR data for **[6]**[B(C₆F₅)₄]⁻ agree with the proposed formulation. ¹H and ¹⁹F 2D DOSY NMR data are consistent with dissociated **[6]**⁺ and [B(C₆F₅)₄]⁻ ions in CD₂Cl₂ at room temperature (see Supporting Information). In particular, the ¹⁹F 2D DOSY NMR data agree with two distinct molecular entities under the studied conditions with hydrodynamic volumes of 2213 Å and 1094 Å, which matches well the respective volumes of [IPr*-ZnC₆F₅]⁺ and [B(C₆F₅)₄]⁻ (from solid state data).



Scheme 2. Synthesis of the Zn-C₆F₅ cation **[6]**⁺

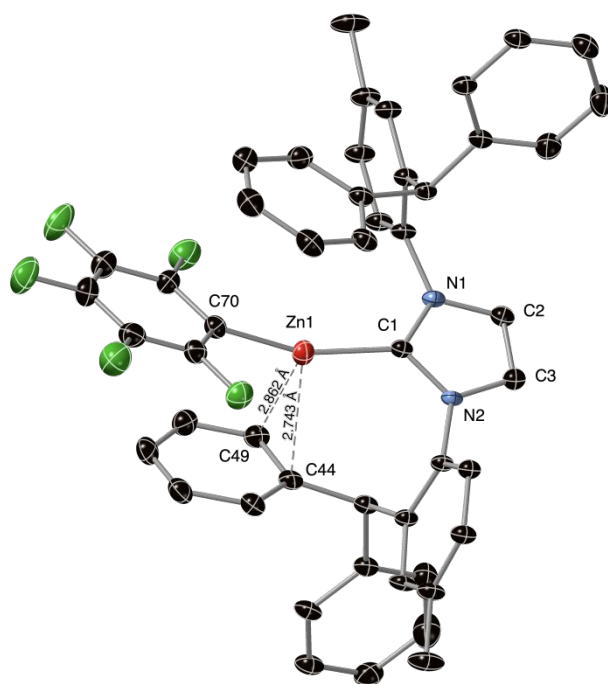


Figure 5. Molecular structure (ORTEP view) of Zn cation [(IPr*)Zn-C₆F₅]⁺. For clarity, two N-CHPh₂ substituents are not represented. Selected bond distances (Å) and angles (°). Zn1-C1 = 1.953(4), C1-N1 = 1.348(5), C1-N2 = 1.358(5), Zn1-C70 = 1.930(4), C70-Zn1-C1 = 160.4(2).

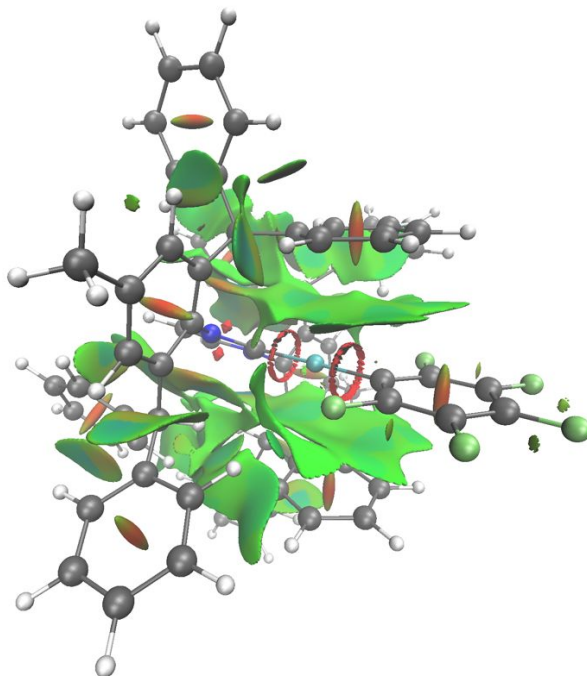


Figure 6. Non covalent interactions (NCI) isosurface ($h = 0.65$) for model cation [(IPr*)Zn-C₆F₅]⁺ (VI), as estimated by DFT calculations at the wB97XD/6-31+G** theory level. Green areas correspond to attractive Van der Waals interactions and red areas indicate repulsive steric congestion.

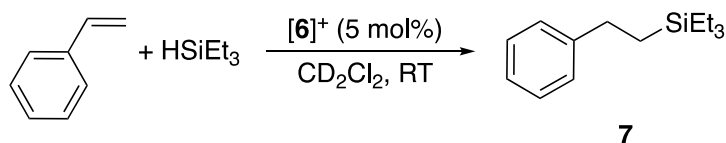
The Lewis acidity of the characterized IPr*-stabilized Zn(II) cations [4-6]⁺ was experimentally evaluated in CD₂Cl₂ using the Gutmann-Beckett method (the ³¹P NMR chemical shift of Et₃P=O Lewis pair adduct is recorded to probe the Lewis acidity and compared to that of free Et₃P=O).^{41,42} According to these measurements, cation [6]⁺ is the strongest Lewis acid of the IPr*-Zn series [Acceptor number (AN) = 55.7, 45.3 and 43.3 for [6]⁺, [4]⁺ and [5]⁺, respectively] and exhibit a comparable Lewis acidity to [(IPr)Zn-C₆F₅]⁺ and landmark Lewis acid B(C₆F₅)₃ [AN = 54.6 and 58.3 for [(IPr)Zn-C₆F₅]⁺ and B(C₆F₅)₃, respectively]. However, the limits of validity of such method are well-known.⁴³ In particular, in the present [IPr*-Zn-R]⁺ systems, the presence of a number of aromatic rings close the Zn(II) center may significantly affect the ³¹P chemical shift of the coordinated O=PEt₃ regardless of the actual Lewis acidity of metal center. Thus, for additional estimation of Lewis acidity, the Fluoride Ion Affinity (FIA) of [4-6]⁺ was also DFT-computed (B3LYP/6-31+G**, PhBr as solvent through a PCM model; see Supporting Information for more details). According to FIA estimations, [IPr*-Zn-C₆F₅]⁺ is indeed the most Lewis acidic IPr*-Zn species ([6]⁺, FIA = 167.7 kJ·mol⁻¹; [4]⁺, FIA = 148.7 kJ·mol⁻¹; [5]⁺, FIA = 147.5 kJ·mol⁻¹) but is significantly less Lewis acidic than [IPr-Zn-C₆F₅]⁺ cation and B(C₆F₅)₃ (FIA = 185.5 and 220.5 kJ·mol⁻¹, respectively).³⁴ Significant steric hindrance around Zn(II) along with its electronic stabilization by p-Ph interactions clearly account for the decreased Lewis acidity at Zn(II) in [IPr*-Zn-C₆F₅]⁺ vs. [IPr-Zn-C₆F₅]⁺.

As stated the Introduction, access to [NHC-Zn-R]⁺ cations with improved hydrolytic stability is a core objective of the present study. The stability of [IPr*-Zn-C₆F₅]⁺ cation towards hydrolysis and O₂ was therefore estimated under controlled conditions and compared to that of the less sterically protected [IPr-Zn-C₆F₅]⁺ cationic analogue. As monitored by ¹H and ¹⁹F NMR, the reaction of [IPr*-Zn-C₆F₅][B(C₆F₅)₄] (0.01 M in C₆D₅Br) with 1 equiv of H₂O at room temperature led to the immediate formation of the corresponding Zn-OH₂ adduct, *i.e.*

$[\text{IPr}^*\text{-Zn}(\text{C}_6\text{F}_5)(\text{H}_2\text{O})]^+$, with the presence of an additional singlet assigned to a $\text{H}_2\text{O-Zn}$ moiety ($\delta = 2.49$ ppm; for comparison, $\delta = 1.29$ ppm for free H_2O in $\text{C}_6\text{D}_5\text{Br}$). Remarkably, such an organozinc cationic water adduct is stable for the studied conditions, with no apparent decomposition/hydrolysis reaction after 12 h, as deduced from NMR data (see SI). In sharp contrast, in the presence of one equiv of H_2O , cation $[\text{IPr-Zn-C}_6\text{F}_5]^+$ (0.01 M in $\text{C}_6\text{D}_5\text{Br}$) is completely hydrolyzed within an hour at RT (as evidenced by ^1H and ^{19}F NMR data, see SI) to afford $\text{C}_6\text{F}_5\text{H}$ and unidentified organozinc species. The greater steric and electronic stabilization provided by IPr^* vs. IPr certainly accounts for the improved stability towards hydrolysis.

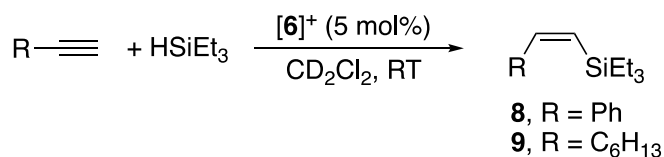
Regarding their reactivity with O_2 , both cations $[\text{IPr}^*\text{-Zn}(\text{C}_6\text{F}_5)(\text{H}_2\text{O})]^+$ and $[\text{IPr-Zn-C}_6\text{F}_5]^+$ (0.01 M in $\text{C}_6\text{D}_5\text{Br}$) exhibit no apparent reaction with O_2 (1 bar) at room temperature after 24 h as monitored by ^1H and ^{19}F NMR.

Styrene and alkyne hydrosilylation catalysis with cations [4-6]⁺. The prepared Zn cations were initially tested for alkene/alkyne hydrosilylation catalysis since examples of Zn-catalysed/initiated alkene/alkyne hydrosilylation remain rare to date.^{44,34,45} At room temperature (in CD_2Cl_2) or 90 °C (in $\text{C}_6\text{D}_5\text{Br}$), cations [4-6]⁺ showed no catalytic activity in 1-hexene hydrosilylation using HSiEt_3 or PhSiH_3 as a silane source. Given that such process likely operates through Lewis-acid type catalysis, the lower Lewis acidity of [4-6]⁺ vs. $[\text{IPr-Zn-C}_6\text{F}_5]^+$ most likely explains the absence of activity. However, cation [6]⁺ (5 mol%) slowly hydrosilylates styrene at room temperature in the presence of HSiEt_3 to the corresponding *anti*-Markovnikov product **7** (Scheme 3), albeit with poor activity (70 % conversion to **7** after 4 days). ^1H NMR monitoring of the catalysis agree with cation [6]⁺ retaining its integrity as the reaction proceeds, in line with a Lewis-acid-type catalysis. Interestingly, under identical conditions, the more Lewis acidic $[\text{IPr-Zn-C}_6\text{F}_5]^+$ cation (5 mol%) polymerizes styrene within a few hours (CD_2Cl_2 , RT, 5 h, quantitative styrene conversion to atactic polystyrene) and no hydrosilylation product was observed.



Scheme 3. Styrene hydrosilylation catalysis by cation $[6]^+$

Cation $[6]^+$ (5 mol%) is also active in alkyne (phenylacetylene and 1-octyne) hydrosilylation to afford the *Z*-selective *anti*-Markovnikov products **8** and **9**, respectively (Scheme 4),^{46,47} albeit with moderate activity (53% and 70 % conversion to **8** and **9**, respectively, after 24 h in CD_2Cl_2). Here again, catalyst $[6]^+$ is stable and not consumed as the catalysis occurs, in line with $[6]^+$ acting a Lewis acid catalyst. In addition, the much higher activity of stronger Lewis acid $[(IPr)Zn-C_6F_5]^+$ under identical conditions (quantitative formation of **8** and **9** within 10 min, CD_2Cl_2 , RT) further hints at a Lewis-acid-mediated process.

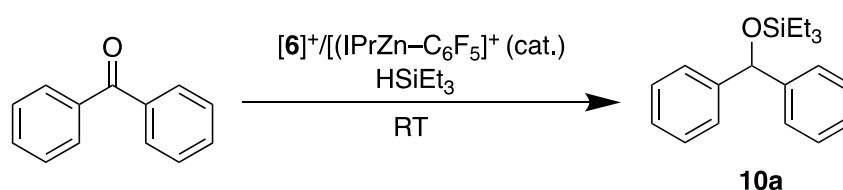


Scheme 4. Alkyne hydrosilylation catalyzed by cation $[6]^+$

Carbonyls and CO₂ hydrosilylation Catalysis by cations [4-6]⁺. Zinc-mediated/catalyzed hydrosilylation of carbonyls such as ketones and aldehydes is well-established in the literature,⁴⁸ though the use of well-defined Zn complexes for such catalysis remains rather limited.^{49,50,51,52,53,54,55} Cationic Zn complexes have rarely been explored as ketone and aldehyde hydrosilylation catalysts: with the exception of strongly Lewis acidic “pseudo-naked” Zn^{2+} of the type $Zn[X]_2$ (X = carborate, ammoniododecaborate),^{56,57} they all consist of $Zn-H$ cationic complexes that perform such catalysis through a coordination/insertion/*s*-bond metathesis sequence.^{58,31,59,60}

The zinc alkyl cations $[4-6]^+$ and $[(IPr)Zn-C_6F_5]^+$ cation were tested in ketone/aldehyde hydrosilylation as potential Lewis acidic catalysts. Benzophenone was initially used as a model substrate in the presence of $HSiEt_3$, and the results are compiled in Table 1. While the Zn alkyl cations $[4]^+$ and $[5]^+$ displayed no hydrosilylation activity (room temperature or 60 °C for prolonged time), the more Lewis acidic $[6]^+$ proved to be highly effective at room temperature. Thus, complete conversion of a 1/1 $Ph_2C=O/HSiEt_3$ to the corresponding mono-hydrosilylated product $Ph_2CHOSiEt_3$ (**10a**) is achieved within 30 min at RT using $[6]^+$ (5 mol %) as catalyst (entries 1 and 2, Table 1). Conversely and contrasting with the reactivity trend observed in alkene/alkyne hydrosilylation, $[(IPr)Zn-C_6F_5]^+$ is significantly less effective with no activity at room temperature (after 24 h), but the quantitative formation of product **10a** is observed after 6 h at 60 °C (entries 3 and 4, Table 1). The selectivity in mono-hydrosilylated product **10a** is also retained in the presence of excess $HSiEt_3$ using catalyst $[6]^+$ with no formation of the over-/double-reduction product, $PhCH_2Ph$ (**11**), over prolonged time (RT and 60 °C). Catalyst $[6]^+$ is also efficient at lower loadings such as 2% and 1% mol (entries 6-8, Table 1). Thus, 86 equiv of $Ph_2C=O$ may be converted to **10a** within 30 min at room temperature (TOF = 172 h⁻¹) in the presence of $HSiEt_3$ and $[6]^+$ (1% mol), and complete conversion is reached after 2 h (entries 7 and 8, Table 1). Further increase in benzophenone feed ratio to 1000/1 (0.1% mol of $[6]^+$) also allowed the quantitative formation of **10a** within 6 h at 60 °C (entry 9, Table 1). Overall, these results suggest that Lewis acidic cation $[6]^+$ stands as an effective and robust ketone hydrosilylation catalyst under mild conditions.

Table 1. Hydrosilylation of benzophenone by $HSiEt_3$ catalyzed by $[6]^+$ and $[(IPr)Zn-C_6F_5]^+$ cations.^a



Entry	Cat. (mol %)	T (°C)	t (h)	NMR yield (%) ^a	TOF (h ⁻¹)
1	[6] ⁺ (5)	25	0.5	100	40
2	[6] ⁺ (5) ^c	25	0.5	100	40
3	[(IPr)Zn-C ₆ F ₅] ⁺ (5) ^c	25	24	0	0
4	[(IPr)Zn-C ₆ F ₅] ⁺ (5) ^c	60	6	100	3.3
5	[6] ⁺ (5) ^d	25 and 60	24 + 2	100	40
6	[6] ⁺ (2) ^c	25	0.5	98	98
7	[6] ⁺ (1)	25	0.5	86	172
8	[6] ⁺ (1)	25	2	100	50
9	[6] ⁺ (0.1)	60	6	100	167

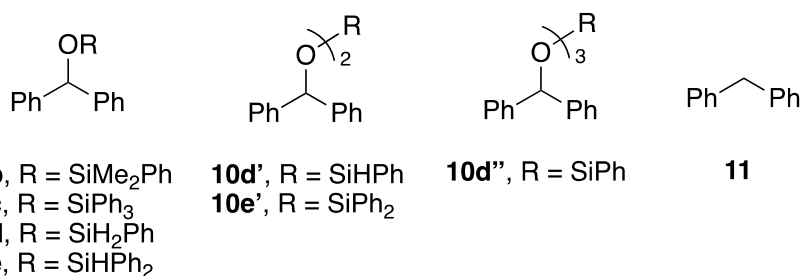
^a Conditions for a typical run: [Cat]₀ = 0.0174 M, C₆D₅Br (unless indicated otherwise). ^b NMR yield in the mono-reduction product **10a**, as determined by ¹H NMR analysis using 4-fluorotoluene as internal reference. ^c CD₂Cl₂ as solvent. ^d A 1/2 Ph₂C=O/HSiEt₃ initial ratio was used.

To further probe the reactivity of cation [**6**]⁺, hydrosilanes scope in benzophenone hydrosilylation catalyzed by [**6**]⁺ (2% mol) was also conducted, and the results are summarized in Table 2. Silane HSiMe₂Ph performs similarly to HSiEt₃ with the quantitative formation of the corresponding hydrosilylation product, Ph₂CHO-SiMe₂Ph (**10b**), within 1 h at room temperature (entry 1, Table. 2). In contrast, the use of silane HSiPh₃ only led to a 17% conversion to Ph₂CHO-SiPh₃ (**10c**) under identical conditions, likely due to its high steric hindrance (entry 2, Table 2). Also, no hydrosilylation was observed with HSi(OEt)₃ as a Si-H source due its poor stability in the presence of [**6**]⁺.⁶¹ The use of hydrosilanes bearing several Si-H moieties such as H₃SiPh and H₂SiPh₂ significantly modified products outcome. Thus, a 1/1 H₃SiPh/Ph₂C=O mixture was quantitatively and selectively converted to diphenylmethane

(**11**), the double reduction product of Ph₂C=O, within 30 min at room temperature (entry 4, Table 2). The formation of **11** likely occurs through the initial formation of hydrosilylation products of the type (Ph₂CHO)_xSiH_{3-x}Ph (x = 1 to 3; **10d**: Ph₂CHO-SiH₂Ph; **10d'**: (Ph₂CHO)₂SiHPh; **10d''**: (Ph₂CHO)₃SiPh; none were observed), that undergo deoxygenation reactions mediated by Lewis acid [6]⁺ leading to the formation of **11** and siloxanes by-products, as previously observed in carbonyls hydrosilylation mediated by strong Lewis acids (entry 5, Table 2).^{56,62,63} Hydrosilylation starting with a 1/3 H₃SiPh/Ph₂C=O ratio, *i.e.* with one Si-H moiety per carbonyl, quantitatively led to a mixture of (Ph₂CHO)_xSiH_{3-x}Ph and **11** in a roughly 1/1 ratio, in line with the limited stability of species (Ph₂CHO)_xSiH_{3-x}Ph and their ready conversion to **11** under the reaction conditions. A similar reactivity trend is observed for benzophenone hydrosilylation performed with H₂SiPh₂ as a Si-H source (entries 6 and 7, Table 2), but the corresponding reduction products of the type (Ph₂CHO)_xSiH_{2-x}Ph₂ (x = 1, 2; **10e**: Ph₂CHO-SiHPh₂; **10e'**: (Ph₂CHO)₂SiPh₂) exhibit improved stability towards Lewis acid-mediated deoxygenation. Overall, mono-hydride silane such as HSiEt₃ and HSiMe₂Ph appear best suited for the fast and selective formation of silyl ether products using Lewis acid [6]⁺.

Table 2. Hydrosilane scope for benzophenone hydrosilylation catalysis using Zn cation [6]⁺.^a

Entry	Silane	t (h)	Ph ₂ C=O Conv. (%)	NMR Yield in 10 (%) ^b	NMR Yield in 11 (%) ^b
1	HSiMe ₂ Ph	1	100	99 (10b)	-
2	HSiPh ₃	1	17	17 (10c)	-



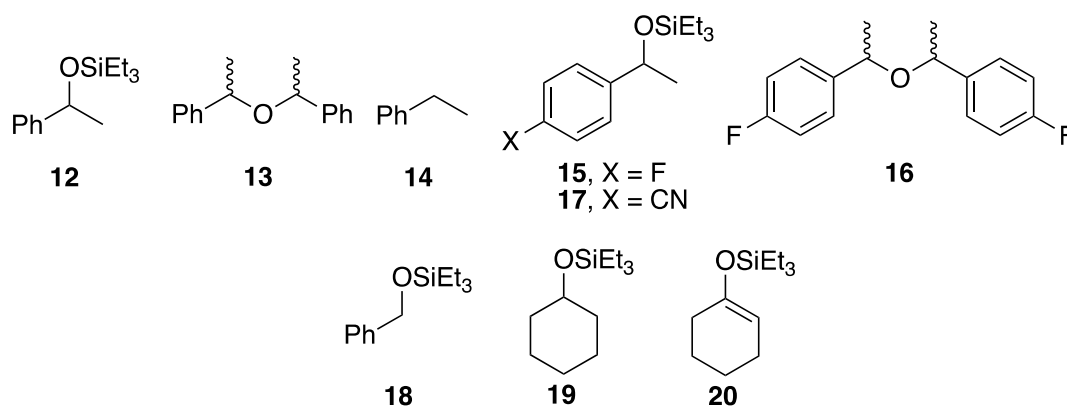
3	HSi(OEt) ₃	1	0	-	-
4	H ₃ SiPh	0.5	100	-	100
5 ^c	H ₃ SiPh	0.5	100	54 (10d+10d'+10d'')	46
6	H ₂ SiPh ₂	0.5	100	16 (10e+10e')	84
7 ^d	H ₂ SiPh ₂	0.5	100	100 (10e+10e')	-

^a Conditions: NMR scale reaction, 2 mol % of **[6]**[B(C₆F₅)₄] ([Cat]₀ = 0.007 M), ratio [Ph₂C=O]₀/[Silane]₀/[Cat]₀ = 50/50/1 (unless specified otherwise), C₆D₅Br, RT. ^b NMR yields in all reduction products were determined by ¹H NMR analysis using 4-fluorotoluene as internal reference. ^c A 3/1 Ph₂C=O/H₃SiPh ratio was used. ^d A 2/1 Ph₂C=O/H₂SiPh₂ ratio was used.

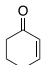
Following silane scope, the ability of cation **[6]**⁺ to hydrosilylate various ketones/aldehyde was evaluated using HSiEt₃ as a silane source. The results are summarized in Table 3. In the presence of HSiEt₃ and **[6]**⁺ (5 mol %), aromatic ketones such as acetophenone and *p*-fluoroacetophenone are readily reduced to the corresponding silyl ethers **12** and **15**, respectively, as the major products, with 90% and 100% ketone conversion as well as complete silane consumption within 30 min at room temperature (entries 1 and 2, Table 3), as deduced from ¹H NMR and GC-MS analysis. Both catalysis also produce the ether products **13** and **16**, respectively (along with Et₃SiOSiEt₃), as minor products (5% and 35% yield, respectively). Such a reductive etherification reaction leading to **13** and **16** is well-known to occur in acid-mediated organosilane reduction of ketones/aldehydes.⁶⁴ The reduction of acetophenone also produces minor amount of doubly reduced product ethylbenzene (**14**). In contrast, hydrosilylation of *p*-cyanoacetophenone and benzaldehyde proceed much slower to selectively afford the mono-reduction products **17** and **18**, respectively (entries 3 and 4, Table 3). Those substrates likely form very robust adducts of the type [(NHC)Zn(C₆F₅)(L)]⁺, L = ketone/aldehyde) upon coordination to **[6]**⁺: given that Zn-L dissociation appears required for hydrosilylation to occur (*vide infra*, DFT calculations), decreased catalytic activity is expected

with more stable $[(\text{NHC})\text{Zn}(\text{C}_6\text{F}_5)(\text{L})]^+$ adducts. Aliphatic ketones such as cyclohexanone may also be efficiently reduced using cation $[\mathbf{6}]^+$ with a nearly complete conversion to the corresponding silylether **19** within 30 min at room temperature (entry 5, Table 3), while the reduction of conjugated ketone 2-cyclohexen-1-one is significantly slower to selectively and quantitatively afford the 1,4 hydrosilylation product **20** after 22 h at room temperature (entry 6, Table 3).

Table 3. Ketone/aldehyde scope in hydrosilylation catalysis with HSiEt_3 catalyzed by Zn cation $[\mathbf{6}]^+$.^a



Entry	Substrate	t (h)	Conv. (%) ^b	Yield (NMR) (%) ^c	Selectivity
1		0.5	90	70 (12+13+14)	12/13/14 ratio: 86/7/7
2		0.5	100	100 (15+16)	15/16 ratio: 65/35
3		24	48	48 (17)	N/A
4		2	19	19 (18)	N/A
5		0.5	100	97 (19)	N/A

6		22	100	100 (20)	N/A
---	---	----	-----	-------------------	-----

^a Conditions: NMR scale reaction, 5 mol % of **[6]**[B(C₆F₅)₄] ([Cat]₀ = 0.007 M), ratio [Ph₂C=O]₀/[HSiEt₃]₀/[Cat]₀ = 20/20/1, CD₂Cl₂, room temperature. ^b Ketone/aldehyde consumption. ^c Calculated by ¹H NMR vs. an internal standard (4-fluorotoluene).

Control experiments and DFT calculations for mechanistic insights on ketone hydrosilylation catalysis by **[6]⁺.** Benzophenone hydrosilylation catalyzed by **[6]**[B(C₆F₅)₄] was further studied as representative of these Lewis-acid-type hydrosilylation catalysis. ¹H NMR monitoring of a 1/10/10 **[6]**[B(C₆F₅)₄]/HSiEt₃/Ph₂C=O catalysis showed that the benzophenone adduct [(IPr*)Zn(C₆F₅)(O=CPh₂)]⁺ (**[21]**⁺) is the only observable Zn species as the catalysis proceeds, thus the likely resting state of the process. Further, salt **[21]**[B(C₆F₅)₄] was isolated as a yellow solid from the latter catalytic run, and its identity was deduced from ¹H, ¹³C and 2D NMR analysis, which are consistent with benzophenone coordination to the Zn center. The independent NMR-scale generation of adduct **[21]**[B(C₆F₅)₄] by reaction of **[6]**[B(C₆F₅)₄] with 1 equiv of benzophenone (CD₂Cl₂, room temperature) further confirmed its identity. Also, a 1/10/10 **[21]**[B(C₆F₅)₄]/HSiEt₃/Ph₂C=O catalysis led to an identical outcome and catalytic activity to that performed with **[6]**[B(C₆F₅)₄], in line with cation **[21]**⁺ being the catalyst resting in these hydrosilylation reactions.

To gain additional insight, a possible mechanism of benzophenone hydrosilylation catalysis by **[6]**⁺ was studied through DFT computation at the wB97XD/6-31+G** theory level using a QMMM approach (see Supporting Information for further details). The proposed DFT-estimated mechanism is depicted in Figure 7, starting from the experimentally observed benzophenone adduct of cation **[6]**⁺ (model **XXI**). From **XXI**, a direct attack of HSiEt₃ on the coordinated benzophenone in **XXI** was initially computed (see Supporting Information, Fig. S52), but such an approach only led to an unrealistically high barrier (> 40 kcal.mol⁻¹). Rather, as shown in Figure 7, an initial dissociation of **XXI** (ΔG = -13 kcal.mol⁻¹) in the presence of

HSiEt₃ appears required to afford the corresponding Et₃SiH-Zn adduct **XXII** along with free benzophenone ($\Delta G = 5.4$ kcal.mol⁻¹). Model **XXII** is only a fleeting intermediate that may react fast through a backside nucleophilic attack of benzophenone at Si-H proceeding at little energy cost through transition state **TS1** ($\Delta G = 16.3$ kcal.mol⁻¹) to afford the benzophenone silylium cation **XXIII** and the neutral Zn-H species (IPr*)Zn(H)(C₆F₅), **XXIV** ($\Delta G = 7.3$ kcal.mol⁻¹). The latter is unstable and further reacts through a hydride transfer from the Zn to the Si center (via **TS2**, $\Delta G = 10.6$ kcal.mol⁻¹) to afford reduction product Ph₂CHOSiEt₃ (**XXV**), the most thermodynamically stable species of the reaction, and re-generate catalyst [(IPr*)Zn-C₆F₅]⁺.

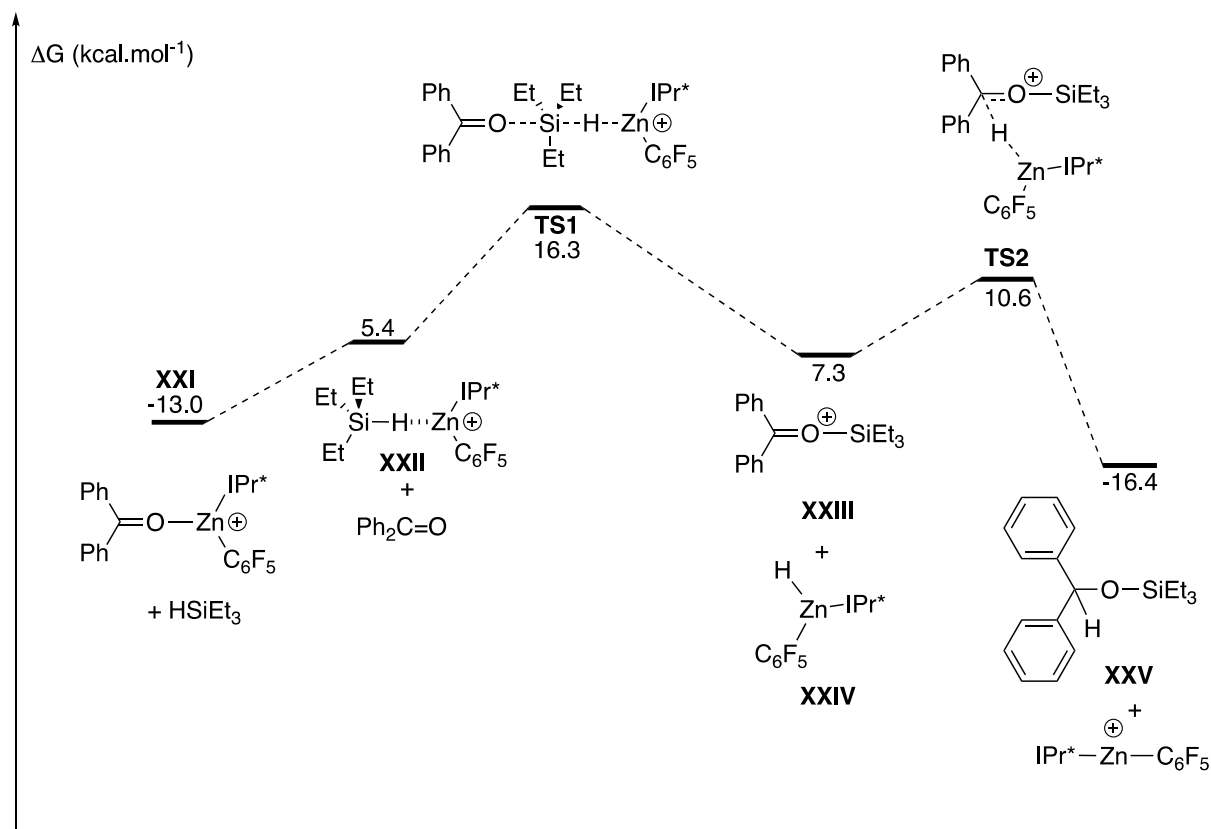


Figure 7. DFT-estimated mechanism of benzophenone hydrosilylation catalyzed by Zn cation [6]⁺ (wB97XD/6-31+G** theory level). Solvent (PhBr) effects were considered by mean of a PCM.

The overall hydrosilylation reaction is thus clearly thermodynamically driven and may readily occur at low energy cost *via* successive transition states **TS1** and **TS2** from trace amount of Et₃SiH-Zn adduct **XXII** that continuously form. Access to silane adduct **XXII** thus appears

crucial for the catalysis to operate but its formation requires dissociation of the benzophenone cationic adduct: in that regard, this may rationalize the lower catalytic activity of the more Lewis acidic [(IPr)Zn-C₆F₅]⁺ Zn cation, which forms a more robust [(IPr)Zn(C₆F₅)(O=CPh₂)]⁺ adduct than less prone to dissociation than the more sterically hindered [(IPr*)Zn(C₆F₅)(O=CPh₂)]⁺. For the less Lewis acidic Zn-alkyl cations [4]⁺ and [5]⁺, the absence of activity probably reflects the absence of any silane activation by such cations. Overall, such mechanism is reminiscent to that proposed and established by Piers in B(C₆F₅)₃-catalyzed hydrosilylation of ketones.^{65,66,67}

The present hydrosilylation mechanism thus proposes the formation of Ph₂C=O-stabilized silylium **XXIII** as an intermediate, raising the question of an actual silylium-catalyzed process in which the Zn cation [(IPr*)Zn-C₆F₅]⁺ would only act as an initiator for the generation of [Ph₂C=O-SiEt₃]⁺, a possible catalyst on its own. To probe this issue further, benzophenone hydrosilylation catalyzed by [Et₃Si]⁺ was DFT-computed (see Supporting Information, Figures S56 and S57): however, the formation of the doubly reduced product (PhCH₂Ph from Ph₂CH-OSiEt₃) is estimated to be significantly faster than the initial reduction of benzophenone to Ph₂CH-OSiEt₃, which should limit selectivity in Ph₂CH-OSiEt₃. In line with the latter, a control ¹H NMR monitoring experiment of a 1/100/100 [Ph₃C][B(C₆F₅)₄]/HSiEt₃/Ph₂C=O mixture (CD₂Cl₂, room temperature) led to a 2/1 Ph₂CH-OSiEt₃/PhCH₂Ph mixture within 40 min along with complete HSiEt₃ consumption. In contrast, as earlier discussed, Zn cation [6]⁺ (1% mol) is a selective catalyst for quantitative Ph₂CH-OSiEt₃ formation under identical catalytic conditions (entry 7, Table 1). Computational and experimental data are thus overall consistent with a Zn-catalyzed Ph₂C=O hydrosilylation process.

CO₂ hydrosilylation catalysis by cation [6]⁺. Cations [4-6]⁺ were also tested in CO₂ hydrosilylation catalysis given the current interest of such transformation and the ability of

strong Lewis acids for catalytic CO₂ functionalization in the presence of hydrosilanes.⁶⁸ While inactive at room temperature, cation [6]⁺ (1 mol %) selectively reduces CO₂ (1.5 bar) to methane (C₆D₅Br, 90 °C) with 80% conversion after 24 h, a comparable activity to Zn cation [(IPr)Zn–C₆F₅]⁺.³⁴ The less Lewis acidic cations [4]⁺ and [5]⁺ displayed moderate activity under such conditions (14% HSiEt₃ conversion to a 1/1 MeOSiEt₃/CH₄ mixture after 24 h). The Zn cation [6]⁺ retained its integrity as the CO₂ reduction proceeds, consistent with a Lewis-acid-type mechanism as that observed and described for [(IPr)Zn–C₆F₅]⁺.³⁴

Conclusion

The present study first showed that two-coordinate **organozinc cations** of the type [(NHC)Zn–R]⁺ incorporating a “bulky-yet-flexible” NHC such as IPr* may be accessible as extremely robust electrophilic species. The steric protection provided by such NHC ligand significantly improves the hydrolytic stability, with the more Lewis acidic cation of the series (*i.e.* [(IPr*)Zn–C₆F₅]⁺) **being significantly more stable towards hydrolysis than benchmark** [(IPr)Zn–C₆F₅]⁺. Electronic stabilization of the Zn(II) center through arene π donation center may also provide substantial electronic stabilization as deduced from structural data for [(IPr*)Zn–C₆F₅]⁺. As a result, IPr*-stabilized Zn(II) cations are less Lewis acidic than (IPr)Zn analogues, but display a distinct and complementary reactivity in catalysis. Thus, while exhibiting no to moderate activity in alkene/alkyne hydrosilylation (unlike highly active [(IPr)Zn–C₆F₅]⁺), [(IPr*)Zn–C₆F₅]⁺ is a highly effective and selective catalyst in ketone hydrosilylation and performs much better than [(IPr)Zn–C₆F₅]⁺. As observed with several other metal centers, the use of IPr* as a supporting NHC ligand in Zn(II) coordination chemistry may well be complementary to that of classically used NHCs.¹³ The latter along with the ready accessibility, **improved hydrolytic stability**, and ability to activate polar substrates of these well-defined Zn-based organocations may promote their further use in catalysis.

Experimental Section

Material, Reagents, and Experimental Methods. All experiments were performed under inert atmosphere using standard glove box or Schlenk techniques. Solvents were freshly distilled under N₂ following standard procedures or dispensed from a commercial purification system and then stored over 4 Å molecular sieves. Deuterated solvents were used as received and stored over 4 Å molecular sieves. NMR spectra were recorded on Bruker Advance I-300 MHz, Bruker Advance III-400 MHz, Bruker Advance II-500 MHz, and Bruker Advance III-600 MHz spectrometers. NMR chemical shift values were determined relative to the residual protons in C₆D₆, C₆D₅Br and CD₂Cl₂ as internal reference for ¹H (δ of the most downfield signal = 7.16, 7.29, 5.32 ppm) and ¹³C{¹H} (δ of the most downfield signal = 128.06, 130.92, 53.84 ppm). ZnMe₂, ZnEt₂, and [CPh₃][B(C₆F₅)₄] were obtained from Strem Chemicals. B(C₆F₅)₃ was obtained from TCI Europe and recrystallized from cold pentane prior to use. The free carbene IPr* was prepared according to the literature^{12,19,69} using an improved procedure to synthesize the diazadiene precursor.⁷⁰

IPr*ZnMe₂ (1). At room temperature, to a colorless solution of IPr* free carbene (0.274 g, 0.30 mmol, 1 eq) in toluene (2 mL) was added dropwise a colorless solution of dimethylzinc (27 μL, 0.39 mmol, 1.3 eq) in toluene (2 mL), resulting in a colorless solution that was stirred for 2 h. Then the solvent was evaporated under vacuum until the reaction mixture turned to a saturated solution, then pentane was slowly added to crystallize at -35 °C in a mixture of toluene and pentane (1:2). **1** was obtained as white crystalline powder after drying under vacuum (0.257 g, 85 % yield). Anal. Calcd for C₇₁H₆₂N₂Zn: N, 2.78; C, 84.55; H 6.20. Found: N, 2.58; C, 84.22; H 6.85. ¹H NMR (500 MHz, C₆D₆): δ (ppm) 7.38 (d, J = 7.4 Hz, 8H, CH-Ar), 7.16 (t, J = 7.6 Hz, 8H, CH-Ar), 7.08 (s, 4H, CH-Ar), 7.06 – 7.00 (m, 12H, CH-Ar), 6.97-6.91 (m, 12H, CH-

Ar), 5.72 (s, 2H, N-CH=CH-N), 5.67 (s, 4H, *CHPh*₂), 1.75 (s, 6H, Me), -0.64 (s, 6H, ZnMe₂).
¹³C NMR (126 MHz, C₆D₅Br): δ (ppm) 188.56 (C_{carbene}), 143.94 (C-Ar), 142.54 (C-Ar), 140.76 (C-Ar), 138.86 (C-Ar), 134.77 (C-Ar), 130.00 (CH-Ar), 129.92 (CH-Ar), 129.23 (CH-Ar), 128.52 (CH-Ar), 128.35 (CH-Ar), 126.69 (CH-Ar), 126.60 (CH-Ar), 122.92 (N-CH=CH-N), 51.57 (*CHPh*₂), 21.20 (Me), -6.85 (ZnMe₂).

IPr*ZnEt₂ (2). At room temperature, to a colorless solution of IPr* free carbene (0.274 g, 0.30 mmol, 1 eq) in toluene (2 mL) was added dropwise a colorless solution of diethylzinc (41 μL, 0.39 mmol, 1.3 eq) in toluene (2 mL), resulting in a colorless solution that was stirred for 2 h. Then the solvent was evaporated under vacuum until the reaction mixture turned to a saturated solution, then pentane was slowly added to crystallize at -35 °C in a mixture of toluene and pentane (1:2). **2** was obtained as white crystalline powder after drying under vacuum (wash with *n*-pentane if necessary) (0.249 g, 80%). Anal. Calcd for C₇₃H₆₆N₂Zn: N, 2.70; C, 84.57; H 6.42. Found: N, 2.70; C, 83.83; H 6.33. ¹H NMR (500 MHz, C₆D₆): δ (ppm) 7.40 (d, J = 7.2 Hz, 8H, CH-Ph), 7.18 (t, J = 7.6 Hz, 8H, CH-Ph), 7.08 (s, 4H, CH-Ar), 7.04 (t, J = 7.3 Hz, 4H, CH-Ph), 6.99 (d, J = 6.8 Hz, 8H, CH-Ph), 6.94 – 6.86 (m, 12H, CH-Ph), 5.74 (s, 4H, *CHPh*₂), 5.64 (s, 2H, N-CH=CH-N), 1.80 (t, J = 8.0 Hz, 6H, ZnCH₂CH₃), 1.75 (s, 6H, Me), 0.18 (q, J = 8.0 Hz, 4H, ZnCH₂CH₃). ¹³C NMR (126 MHz, C₆D₆):⁷¹ δ (ppm) 144.38 (C-Ar), 143.66 (C-Ar), 141.37 (C-Ar), 139.47 (C-Ar), 130.56 (C-Ar), 130.51 (CH-Ar), 129.76 (CH-Ar), 128.95 (CH-Ar), 128.66 (CH-Ar), 127.10 (CH-Ar), 126.76 (CH-Ar), 123.01 (N-CH=CH-N), 52.09 (*CHPh*₂), 21.31 (Me), 15.08 (ZnCH₂CH₃), 6.44 (ZnCH₂CH₃).

IPr*ZnPh₂ (3). At room temperature, to a colorless solution of IPr* free carbene (0.457 g, 0.50 mmol, 1 eq) in toluene (8 mL) was added dropwise a colorless solution of diphenyl zinc (0.110 g, 0.50 mmol, 1 eq) in toluene (4 mL), resulting in an off-white solution that was stirred for 2 h at room temperature. Then the solvent was evaporated under vacuum until the reaction

mixture turned to a saturated solution, then pentane was slowly added to recrystallize at -35 °C in a mixture of toluene and pentane (1:2). IPr*ZnPh₂ was obtained as white crystalline powder after drying under vacuum (wash with *n*-pentane if necessary) (0.424 g, 75%). ¹H NMR (400 MHz, C₆D₆): δ (ppm) 7.36 – 7.30 (m, 4H, CH-Ar), 7.24 – 6.80 (m, 50H, CH-Ar), 5.80 (s, 4H, CHPh₂), 5.59 (s, 2H, N-CH=CH-N), 1.85 (s, 6H, Me). ¹³C NMR (126 MHz, C₆D₆): δ (ppm) 185.49 (C_{carbene}), 161.51 (C-Ar), 143.91 (C-Ar), 143.06 (C-Ar), 141.50 (C-Ar), 140.10 (C-Ar), 139.62 (CH-Ar), 135.56 (C-Ar), 131.41 (CH-Ar), 130.50 (CH-Ar), 129.64 (CH-Ar), 129.03 (CH-Ar), 128.68 (CH-Ar), 127.10 (CH-Ar), 126.87 (CH-Ar), 126.86 (CH-Ar), 125.62 (CH-Ar), 123.64 (N-CH=CH-N), 52.32 (CHPh₂), 21.28 (Me).

[IPr*ZnMe][B(C₆F₅)₄] ([4][B(C₆F₅)₄]). At room temperature, to a colorless solution of IPr*ZnMe₂ (0.242 g, 0.24 mmol, 1 eq) in PhF (10 mL) was added dropwise a yellow solution of trityl tetrakis(pentafluorophenyl)borate [CPh₃][B(C₆F₅)₄] (0.221 g, 0.24 mmol, 1 eq) in PhF (10 mL), immediately giving a yellow solution. The reaction mixture was stirred for 2 h at room temperature. The solvent was then evaporated under vacuum and the resulting oily residue was triturated with *n*-pentane (10 x 5 mL) then dried under vacuum to afford a white powder (0.341 g, 85 %). Anal. Calcd for C₉₄H₅₉BF₂₀N₂Zn: N, 1.67; C, 67.50; H 3.56. Found: N, 1.51; C, 67.38; H 3.82. ESI-MS (*m/z*): *Positive* [IPr*ZnMe]⁺¹ (C₇₀H₅₉N₂Zn⁺¹) 991.40 (Calcd); 991.39 (Found); *Negative* [B(C₆F₅)₄]⁻¹ (C₂₄F₂₀B⁻¹) 678.98 (Calcd); 678.98 (Found). ¹H NMR (500 MHz, CD₂Cl₂): δ (ppm) 7.31 (m, 16H, CH-Ar), 7.23 (m, 8H, CH-Ar), 6.91 (s, 4H, CH-Ar), 6.87 (m, 8H, CH-Ar), 6.76 (m, 8H, CH-Ar), 6.18 (s, 2H, N-CH=CH-N), 4.95 (s, 4H, CHPh₂), 2.26 (s, 6H, Me), -0.91 (s, 3H, ZnMe). ¹³C NMR (126 MHz, CD₂Cl₂): δ (ppm) 165.35 (C_{carbene}), 148.53 (dm, *J*_{CF} = 243 Hz, *o*-B(C₆F₅)₄⁻), 142.98 (C-Ar), 142.29 (C-Ar), 141.93 (C-Ar), 141.01 (C-Ar), 138.64 (dm, *J*_{CF} = 247 Hz, *p*-B(C₆F₅)₄⁻), 136.67 (dm, *J*_{CF} = 249 Hz, *m*-B(C₆F₅)₄⁻), 131.60 (CH-Ar), 131.50 (C-Ar), 130.18 (CH-Ar), 129.59 (CH-Ar), 129.48 (CH-Ar), 129.26 (CH-Ar), 128.31 (CH-Ar), 128.21 (CH-Ar), 126.50 (N-CH=CH-N), 51.99 (CHPh₂), 21.95 (Me), -6.83

(ZnMe). ^{19}F NMR (282 MHz, CD_2Cl_2): δ (ppm) -133.10 (br, $o\text{-B}(\text{C}_6\text{F}_5)_4^-$), -163.77 (t, $J_{\text{FF}} = 20$ Hz, $p\text{-B}(\text{C}_6\text{F}_5)_4^-$), -167.60 (bt, $m\text{-B}(\text{C}_6\text{F}_5)_4^-$).

[IPr*ZnEt][B(C₆F₅)₄] ([5][B(C₆F₅)₄]). At room temperature, to a colorless solution of IPr*ZnEt₂ (0.249 g, 0.24 mmol, 1 eq) in PhF (10 mL) was added dropwise a yellow solution of trityl tetrakis(pentafluorophenyl)borate [CPh_3][B(C₆F₅)₄] (0.221 g, 0.24 mmol, 1 eq) in PhF (5 mL), giving a yellow solution immediately. The reaction mixture was stirred for 2 h at room temperature. The solvent was then evaporated under vacuum and the resulting oily residue was triturated with *n*-pentane (10 x 5 mL), dried under vacuum to afford a white powder (0.352 g, 87 %). Crystals were obtained from $\text{CH}_2\text{Cl}_2/n\text{-pentane}$ 1:2 by diffusion at -37°C for 3 days. Anal. Calcd for $\text{C}_{95}\text{H}_{61}\text{BF}_{20}\text{N}_2\text{Zn}$: N, 1.60; C, 68.58; H 3.85. Found: N, 1.47; C, 66.74; H 3.85. ^1H NMR (300 MHz, CD_2Cl_2): δ (ppm) 7.36-7.22 (m, 24H, CH-Ar), 6.88 (s, 4H, CH-Ar), 6.86 (m, 8H, CH-Ar), 6.75 (m, 8H, CH-Ar), 6.10 (s, 2H, N-CH=CH-N), 4.93 (s, 4H, CHPh_2), 2.24 (s, 6H, Me), 0.51 (t, $J = 8.1$ Hz, 3H, ZnCH_2CH_3), -0.02 (q, $J = 8.1$ Hz, 2H, ZnCH_2CH_3). ^{13}C NMR (126 MHz, CD_2Cl_2): δ (ppm) 165.8 ($\text{C}_{\text{carbene}}$), 148.5 (dm, $J_{\text{CF}} = 253$ Hz, $o\text{-B}(\text{C}_6\text{F}_5)_4^-$), 143.0 (C-Ar), 142.44 (C-Ar), 141.9 (C-Ar), 141.0 (C-Ar), 138.6 (dm, $J_{\text{CF}} = 244$ Hz, $p\text{-B}(\text{C}_6\text{F}_5)_4^-$), 136.7 (dm, $J_{\text{CF}} = 244$ Hz, $m\text{-B}(\text{C}_6\text{F}_5)_4^-$), 131.6 (C-Ar), 131.5 (CH-Ar), 130.1 (CH-Ar), 129.6 (CH-Ar), 129.4 (CH-Ar), 129.1 (CH-Ar), 128.2 (CH-Ar), 128.2 (CH-Ar), 126.2 (N-CH=CH-N), 51.9 (CHPh_2), 21.9 (Me), 9.8 (ZnCH_2CH_3), 8.0 (ZnCH_2CH_3). ^{19}F NMR (282 MHz, CD_2Cl_2): δ (ppm) -133.11 (br, $o\text{-B}(\text{C}_6\text{F}_5)_4^-$), -163.79 (t, $J_{\text{FF}} = 20$ Hz, $p\text{-B}(\text{C}_6\text{F}_5)_4^-$), -167.62 (bt, $m\text{-B}(\text{C}_6\text{F}_5)_4^-$).

[IPr*Zn(C₆F₅)][B(C₆F₅)₄] ([6][B(C₆F₅)₄]). At room temperature, to a suspension of [IPr*ZnMe][B(C₆F₅)₄] (0.251 g, 0.15 mmol, 1 eq) in PhF (5 mL) was added dropwise a colorless solution of tris(pentafluorophenyl)borane $\text{B}(\text{C}_6\text{F}_5)_3$ (0.077 g, 0.15 mmol, 1 eq) and triethylsilane Et_3SiH (48 μL , 0.30 mmol, 2 eq) to promote the reaction in PhF (5 mL). The reaction mixture was stirred for 24 h at room temperature, resulting in a colorless solution. The

volatiles were then evaporated under vacuum and the resulting white oily residue was triturated with *n*-pentane (6 x 5 mL) then dried under vacuum to afford a white powder (0.230 g, 84%). Crystals were obtained from CH₂Cl₂ and *n*-heptane by diffusion at -37 °C for 3 days. Anal. Calcd for C₉₉H₅₆BF₂₅N₂Zn: N, 1.52; C, 65.34; H 3.23. Found: N, 1.46; C, 64.22; H 3.27. ¹H NMR (300 MHz, CD₂Cl₂): δ (ppm) 7.31 (m, 12H, CH-Ar), 7.18 (m, 12H, CH-Ar), 7.00 (s, 4H, CH-Ar), 6.85 (m, 16H, CH-Ar), 6.39 (s, 2H, N-CH=CH-N), 5.11 (s, 4H, CHPh₂), 2.32 (s, 6H, Me). ¹³C NMR (126 MHz, CD₂Cl₂): δ (ppm) 165.45 (C_{carbene}), 148.58 (dm, *J*_{CF} = 236 Hz, *o*-B(C₆F₅)₄⁻), 142.76 (C-Ar), 142.44 (C-Ar), 141.99 (C-Ar), 140.65 (C-Ar), 138.62 (dm, *J*_{CF} = 249 Hz, *p*-B(C₆F₅)₄⁻), 136.68 (dm, *J*_{CF} = 249 Hz, *m*-B(C₆F₅)₄⁻), 131.84 (CH-Ar), 131.81 (C-Ar), 130.18 (CH-Ar), 129.54 (CH-Ar), 129.35 (CH-Ar), 129.26 (CH-Ar), 128.29 (CH-Ar), 128.19 (CH-Ar), 126.75 (N-CH=CH-N), 52.38 (CHPh₂), 21.97 (Me). ¹⁹F NMR (282 MHz, CD₂Cl₂): δ (ppm) -117.31 (m, *o*-ZnC₆F₅), -133.13 (br, *o*-B(C₆F₅)₄⁻), -152.75 (t, *J*_{FF} = 18 Hz, *p*-ZnC₆F₅), -160.51 (m, *m*-ZnC₆F₅), -163.79 (t, *J*_{FF} = 20 Hz, *p*-B(C₆F₅)₄⁻), -167.62 (bt, *J*_{FF} = 20 Hz, *m*-B(C₆F₅)₄⁻).

Styrene hydrosilylation catalyzed by species [6][B(C₆F₅)₄]. In a N₂-filled glovebox, an equimolar amount of styrene and HSiEt₃ (140 μmol) and catalyst [6][B(C₆F₅)₄] (7 μmol, 5 mol %) were dissolved in 0.5 mL of C₆D₅Br at room temperature. Hexamethylbenzene (7 μmol), acting as an internal standard, was also added to the mixture. The resulting solution was charged in a J-Young NMR tube. The reaction was monitored by ¹H NMR spectroscopy up to 4 days at RT showing the absence of polystyrene but the slow and selective formation of hydrosilylation product **7**, identified by comparison with literature NMR data.⁷²

Alkyne hydrosilylation catalyzed by species [6][B(C₆F₅)₄]. An equimolar amount of phenylacetylene or 1-octyne and HSiEt₃ (140 μmol) and catalyst [6][B(C₆F₅)₄] (7 μmol, 5 mol %) were dissolved in 0.5 mL in CD₂Cl₂ at room temperature. 4-fluorobenzene (7 μmol), acting

as an internal standard, was also added to the mixture. The resulting solution was charged in a J-Young NMR tube. The reaction was monitored by ^1H NMR spectroscopy showing the quantitative formation of the *Z*-hydrosilylation products **8** or **9**, respectively, as identified by comparison with literature NMR data.^{47,46} The identity of product **8** was further confirmed by GC-MS analysis: $t_{\text{R}} = 5.58$ min, m/z 218.1 (M^+ , Calcd for $\text{C}_{14}\text{H}_{22}\text{Si}^+$: 218.1, Ph-CH=CH-SiEt₃), 189.1 ($\text{M}^+ - 29(\text{Et})$, Calcd for $\text{C}_{12}\text{H}_{17}\text{Si}^+$: 189.1, Ph-CH=CH-SiEt₃).

Benzophenone hydrosilylation catalyzed by species [6][B(C₆F₅)₄] (Tables 1 and 2). In a N₂-filled glovebox, benzophenone (174 μmol , 50 equiv. vs. [6][B(C₆F₅)₄]), the appropriate amount of the desired silane (vs. [6][B(C₆F₅)₄]) and [6][B(C₆F₅)₄] (3.48 μmol) were dissolved in 0.5 mL of C₆D₅Br. One equivalent of 4-fluorotoluene (3.48 μmol), acting as an internal standard, was also added to the mixture. The resulting solution was charged in a J-Young NMR tube. The catalytic reaction was monitored by ^1H NMR spectroscopy for the appropriate time leading to the formation of the corresponding reduction products (see Table 2), which were identified by comparison of the ^1H NMR data with those of the literature.^{73,74,75,76,77,78} Products yield and relative ratio were determined by ^1H NMR spectroscopy with 4-fluorotoluene as internal standard.

Ketone/aldehyde scope in hydrosilylation catalysis by species [6][B(C₆F₅)₄] (Table 3). In a N₂-filled glovebox, the appropriate amount of the desired ketone/aldehyde (174 μmol , 20 equiv. vs. catalyst), HSiEt₃ (174 μmol , 20 equiv. vs. catalyst) and [6][B(C₆F₅)₄] (3.48 μmol) were dissolved in 0.5 mL of CD₂Cl₂. One equivalent of 4-fluorotoluene (3.48 μmol), acting as an internal standard, was also added to the mixture. The resulting solution was charged in a J-Young NMR tube. The catalytic reaction was monitored by ^1H NMR spectroscopy for the appropriate time leading to the formation of the corresponding reduction products, which were identified by comparison of the ^1H NMR data with those of the literature.^{79–82, 81,83,84,85,86} Except for cyclohexanone and 4'-cyanoacetophenone hydrosilylation reactions, GC-MS analysis of all

crude products was also performed and further confirmed ^1H NMR analysis. GC-MS data: *acetophenone hydrosilylation*, $t_{\text{R}} = 4.60$ min, m/z 217.4 ($\text{M}^+ - 29(\text{Et})$, Calcd for $\text{C}_{10}\text{H}_{25}\text{OSi}_2^+$: 217.1, $\text{Et}_3\text{SiOSiEt}_3$); $t_{\text{R}} = 5.28$ min, m/z 207.3 ($\text{M}^+ - 29(\text{Et})$, Calcd for $\text{C}_{12}\text{H}_{19}\text{OSi}^+$: 207.1, **12**); $t_{\text{R}} = 5.85$ min, m/z 211.1 ($\text{M}^+ - 15(\text{Me})$, Calcd for $\text{C}_{15}\text{H}_{15}\text{O}^+$: 211.1, **13**). *4-fluoroacetophenone hydrosilylation*: $t_{\text{R}} = 4.62$ min, m/z 217.4 ($\text{M}^+ - 29(\text{Et})$, Calcd for $\text{C}_{10}\text{H}_{25}\text{OSi}_2^+$: 217.1, $\text{Et}_3\text{SiOSiEt}_3$); $t_{\text{R}} = 5.31$ min, m/z 225.3 ($\text{M}^+ - 29(\text{Et})$, Calcd for $\text{C}_{12}\text{H}_{18}\text{FOSi}^+$: 225.1, **15**); $t_{\text{R}} = 5.86$ min, m/z 247.2 ($\text{M}^+ - 15(\text{Me})$, Calcd for $\text{C}_{15}\text{H}_{13}\text{F}_2\text{O}^+$: 247.1, **16**). *Benzaldehyde hydrosilylation*: $t_{\text{R}} = 4.44$ min, m/z 217.1 ($\text{M}^+ - 29(\text{Et})$, Calcd for $\text{C}_{10}\text{H}_{25}\text{OSi}_2^+$: 217.1, $\text{Et}_3\text{SiOSiEt}_3$); $t_{\text{R}} = 5.30$ min, m/z 193.2 ($\text{M}^+ - 29(\text{Et})$, Calcd for $\text{C}_{11}\text{H}_{17}\text{OSi}^+$: 193.1, **18**). *2-cyclohexen-1-one hydrosilylation*: $t_{\text{R}} = 4.89$ min, m/z 212.3 (M^+ , Calcd for $\text{C}_{12}\text{H}_{24}\text{OSi}^+$: 212.2, **20**).

[IPr*Zn(C₆F₅)(O=CPh₂)] [B(C₆F₅)₄] ([21] [B(C₆F₅)₄]) isolated from a benzophenone hydrosilylation catalysis run using 10 mol% of catalyst [6] [B(C₆F₅)₄]. At room temperature in a N₂-filled glovebox, to a solution of [6] [B(C₆F₅)₄] (31.8 mg, 17.4 μmol, 1 eq) in CD₂Cl₂ (0.5 mL) was added benzophenone (31.7 mg, 17.4 μmol, 10 eq) and HSiEt₃ (28 μL, 17.4 μmol, 10 eq). After 24 hours, the reaction mixture was filtered through Celite. The solvent was evaporated, and the oily residue was triturated with pentane (5 x 3 mL). After drying under vacuum, a yellow powder (29 mg) was collected and analyzed by NMR, indicating the quantitative formation of the benzophenone adduct [21] [B(C₆F₅)₄], which was not further purified. ^1H NMR (400 MHz, CD₂Cl₂): δ (ppm) 7.72 (t, $J = 7.5$ Hz, 2H, CH-Ph), 7.35 (t, $J = 7.5$ Hz, 4H, CH-Ph), 7.25-7.15 (m, 30H, CH-Ar), 7.04 (m, 12H, CH-Ar), 6.80 (m, 8H, CH-Ar), 5.53 (s, 2H, N-CH=CH-N), 5.27 (s, 4H, CHPh₂), 2.24 (s, 6H, Me). ^{13}C NMR (126 MHz, CD₂Cl₂): δ (ppm) 166.85 (C_{carbene}), 148.55 (dm, $J_{\text{CF}} = 238$ Hz, *o*-B(C₆F₅)₄⁻), 143.11 (C-Ar), 142.68 (C-Ar), 141.58 (C-Ar), 141.41 (C-Ar), 138.62 (dm, $J_{\text{CF}} = 244$ Hz, *p*-B(C₆F₅)₄⁻), 136.68 (dm, $J_{\text{CF}} = 245$ Hz, *m*-B(C₆F₅)₄⁻), 136.56 (C-Ar), 136.31 (CH-Ar), 132.42 (C-Ar), 131.47 (CH-

Ar), 131.11 (CH-Ar), 129.91 (CH-Ar), 129.87 (CH-Ar), 129.35 (CH-Ar), 129.21 (CH-Ar), 129.12 (CH-Ar), 127.99 (CH-Ar), 127.92 (CH-Ar), 126.62 (N-CH=CH-N), 52.78 (CHPh₂), 21.87 (Me). ¹⁹F NMR (282 MHz, CD₂Cl₂): δ (ppm) -115.51 (m, *o*-ZnC₆F₅), -133.09 (br, *o*-B(C₆F₅)₄), -153.47 (t, *J*_{FF} = 19 Hz, *p*-ZnC₆F₅), -160.98 (m, *m*-ZnC₆F₅), -163.74 (t, *J*_{FF} = 21 Hz, *p*-B(C₆F₅)₄), -167.58 (bt, *J*_{FF} = 18 Hz, *m*-B(C₆F₅)₄).

Supporting Information: NMR spectra, crystallographic data, DFT calculations, atom coordinates of models (.xyz file).

CCDC 2270481-2270484 and 2270615 contain the supplementary crystallographic data for this paper. These data can be obtained free of charge via www.ccdc.cam.ac.uk/data_request/cif, or by emailing data_request@ccdc.cam.ac.uk, or by contacting The Cambridge Crystallographic Data Centre, 12 Union Road, Cambridge CB2 1EZ, UK; fax: +44 1223 336033.

The authors declare no competing financial interests.

Acknowledgments. The University of Strasbourg and the CNRS are gratefully acknowledged for financial support. X. X. thank the Chinese Scholarship Council (CSC) and the Fondation Jean-Marie Lehn for PhD and post-doctoral fellowships, respectively.

References

- (1) Nolan, S. P. *N-Heterocyclic Carbenes*; Wiley-VCH Verlag GmbH & Co. KGaA, 2014.
- (2) Herrmann, W. A. N-Heterocyclic Carbenes: A New Concept in Organometallic Catalysis. *Angew. Chem. Int. Ed.* **2002**, *41* (8), 1290–1309. [https://doi.org/10.1002/1521-3773\(20020415\)41:8<1290::AID-ANIE1290>3.0.CO;2-Y](https://doi.org/10.1002/1521-3773(20020415)41:8<1290::AID-ANIE1290>3.0.CO;2-Y).
- (3) Nelson, D. J.; Nolan, S. P. Quantifying and Understanding the Electronic Properties of N-Heterocyclic Carbenes. *Chem. Soc. Rev.* **2013**, *42* (16), 6723. <https://doi.org/10.1039/c3cs60146c>.
- (4) Smith, C. A.; Narouz, M. R.; Lummis, P. A.; Singh, I.; Nazemi, A.; Li, C.-H.; Crudden, C. M. N-Heterocyclic Carbenes in Materials Chemistry. *Chem. Rev. Wash. DC U. S.* **2019**, *119* (Copyright (C) 2020 American Chemical Society (ACS). All Rights Reserved.), 4986–5056. <https://doi.org/10.1021/acs.chemrev.8b00514>.
- (5) Zhao, Q.; Meng, G.; Szostak, M.; Nolan, S. P. N-Heterocyclic Carbene (NHC) Complexes in C-H Activation Reactions. *Chem. Rev. Wash. DC U. S.* **2020**, *120* (Copyright (C) 2020 American Chemical Society (ACS). All Rights Reserved.), 1981–2048. <https://doi.org/10.1021/acs.chemrev.9b00634>.
- (6) Hopkinson, M. N.; Richter, C.; Schedler, M.; Glorius, F. An Overview of N-Heterocyclic Carbenes. *Nature* **2014**, *510* (7506), 485–496. <https://doi.org/10.1038/nature13384>.
- (7) Crabtree, R. H. Abnormal, Mesoionic and Remote N-Heterocyclic Carbene Complexes. *Coord. Chem. Rev.* **2013**, *257* (3–4), 755–766. <https://doi.org/10.1016/j.ccr.2012.09.006>.
- (8) Roy, M. M. D.; Omaña, A. A.; Wilson, A. S. S.; Hill, M. S.; Aldridge, S.; Rivard, E. Molecular Main Group Metal Hydrides. *Chem. Rev.* **2021**, *121*, 12784–12965. <https://doi.org/10.1021/acs.chemrev.1c00278>.
- (9) Doddi, A.; Peters, M.; Tamm, M. N-Heterocyclic Carbene Adducts of Main Group Elements and Their Use as Ligands in Transition Metal Chemistry. *Chem. Rev.* **2019**, *119* (12), 6994–7112. <https://doi.org/10.1021/acs.chemrev.8b00791>.
- (10) Roesky, H. W. Chemistry of Low Valent Silicon. *J. Organomet. Chem.* **2013**, *730*, 57–62. <https://doi.org/10.1016/j.jorganchem.2012.08.025>.
- (11) Romain, C.; Bellemin-Laponnaz, S.; Dagorne, S. Recent Progress on NHC-Stabilized Early Transition Metal (Group 3–7) Complexes: Synthesis and Applications. *Coord. Chem. Rev.* **2020**, *422*, 213411. <https://doi.org/10.1016/j.ccr.2020.213411>.
- (12) Berthon-Gelloz, G.; Siegler, M. A.; Spek, A. L.; Tinant, B.; Reek, J. N. H.; Markó, I. E. IPr* an Easily Accessible Highly Hindered N-Heterocyclic Carbene. *Dalton Trans* **2010**, *39* (6), 1444–1446. <https://doi.org/10.1039/B921894G>.
- (13) Izquierdo, F.; Manzini, S.; Nolan, S. P. The Use of the Sterically Demanding IPr* and Related Ligands in Catalysis. *Chem Commun* **2014**, *50* (95), 14926–14937. <https://doi.org/10.1039/C4CC05289G>.

- (14) Vanden Broeck, S. M. P.; Nahra, F.; Cazin, C. S. J. Bulky-Yet-Flexible Carbene Ligands and Their Use in Palladium Cross-Coupling. *Inorganics* **2019**, *7*, 78. <https://doi.org/10.3390/inorganics7060078>.
- (15) Zhao, Q.; Meng, G.; Li, G.; Flach, C.; Mendelsohn, R.; Lalancette, R.; Szostak, R.; Szostak, M. IPr# – Highly Hindered, Broadly Applicable N-Heterocyclic Carbenes. *Chem. Sci.* **2021**, *12* (31), 10583–10589. <https://doi.org/10.1039/D1SC02619D>.
- (16) Ibni Hashim, I.; Scattolin, T.; Tzouras, N. V.; Bourda, L.; Van Hecke, K.; Ritacco, I.; Caporaso, L.; Cavallo, L.; Nolan, S. P.; Cazin, C. S. J. Straightforward Synthesis of [Cu(NHC)(Alkynyl)] and [Cu(NHC)(Thiolato)] Complexes (NHC = N-Heterocyclic Carbene). *Dalton Trans.* **2022**, *51* (1), 231–240. <https://doi.org/10.1039/D1DT03710B>.
- (17) Ibni Hashim, I.; Tzouras, N. V.; Ma, X.; Bourda, L.; Van Hecke, K.; Nolan, S. P.; Cazin, C. S. J. Improved Synthetic Routes to N-Heterocyclic Carbene-Metal-Diketonato Complexes of Gold and Copper. *Dalton Trans.* **2022**, *51* (35), 13246–13254. <https://doi.org/10.1039/D2DT02276A>.
- (18) Dash, C.; Das, A.; Yousufuddin, M.; Dias, H. V. R. Isolable, Copper(I) Dicarbonyl Complexes Supported by N-Heterocyclic Carbenes. *Inorg. Chem.* **2013**, *52* (3), 1584–1590. <https://doi.org/10.1021/ic302455y>.
- (19) Gómez-Suárez, A.; Ramón, R. S.; Songis, O.; Slawin, A. M. Z.; Cazin, C. S. J.; Nolan, S. P. Influence of a Very Bulky N-Heterocyclic Carbene in Gold-Mediated Catalysis. *Organometallics* **2011**, *30* (20), 5463–5470. <https://doi.org/10.1021/om200705y>.
- (20) Scattolin, T.; Voloshkin, V. A.; Martynova, E.; Vanden Broeck, S. M. P.; Beliš, M.; Cazin, C. S. J.; Nolan, S. P. Synthesis and Catalytic Activity of Palladium Complexes Bearing N-Heterocyclic Carbenes (NHCs) and 1,4,7-Triaza-9-Phosphatricyclo[5.3.2.1]Tridecane (CAP) Ligands. *Dalton Trans.* **2021**, *50* (27), 9491–9499. <https://doi.org/10.1039/D1DT01716K>.
- (21) Zhou, T.; Ma, S.; Nahra, F.; Obled, A. M. C.; Poater, A.; Cavallo, L.; Cazin, C. S. J.; Nolan, S. P.; Szostak, M. [Pd(NHC)(μ -Cl)Cl]₂: Versatile and Highly Reactive Complexes for Cross-Coupling Reactions That Avoid Formation of Inactive Pd(I) Off-Cycle Products. *iScience* **2020**, *23* (8), 101377. <https://doi.org/10.1016/j.isci.2020.101377>.
- (22) Izquierdo, F.; Chartoire, A.; Nolan, S. P. Direct S-Arylation of Unactivated Arylsulfoxides Using [Pd(IPr*)(Cin)Cl]. *ACS Catal.* **2013**, *3* (10), 2190–2193. <https://doi.org/10.1021/cs400533e>.
- (23) Chartoire, A.; Lesieur, M.; Falivene, L.; Slawin, A. M. Z.; Cavallo, L.; Cazin, C. S. J.; Nolan, S. P. [Pd(IPr*)(Cinnamyl)Cl]: An Efficient Pre-Catalyst for the Preparation of Tetra-Ortho-Substituted Biaryls by Suzuki–Miyaura Cross-Coupling. *Chem. – Eur. J.* **2012**, *18* (15), 4517–4521. <https://doi.org/10.1002/chem.201104009>.
- (24) Maliszewski, B. P.; Tzouras, N. V.; Guillet, S. G.; Saab, M.; Beliš, M.; Van Hecke, K.; Nahra, F.; Nolan, S. P. A General Protocol for the Synthesis of Pt-NHC (NHC = N-Heterocyclic Carbene) Hydrosilylation Catalysts. *Dalton Trans.* **2020**, *49* (41), 14673–14679. <https://doi.org/10.1039/D0DT03480K>.
- (25) Żak, P.; Bołt, M.; Lorkowski, J.; Kubicki, M.; Pietraszuk, C. Platinum Complexes

Bearing Bulky N-Heterocyclic Carbene Ligands as Efficient Catalysts for the Fully Selective Dimerization of Terminal Alkynes. *ChemCatChem* **2017**, *9* (19), 3627–3631. <https://doi.org/10.1002/cctc.201700580>.

(26) Balogh, J.; Slawin, A. M. Z.; Nolan, S. P. Bulky N-Heterocyclic Carbene IPr* in Selected Organo- and Transition Metal-Mediated Catalytic Applications. *Organometallics* **2012**, *31* (8), 3259–3263. <https://doi.org/10.1021/om300104j>.

(27) Leverett, A. R.; Cole, M. L.; McKay, A. I. An Exceptionally Stable NHC Complex of Indane (InH₃). *Dalton Trans.* **2019**, *48* (5), 1591–1594. <https://doi.org/10.1039/C8DT04956D>.

(28) Specklin, D.; Fliedel, C.; Dagorne, S. Recent Representative Advances on the Synthesis and Reactivity of N-Heterocyclic-Carbene-Supported Zinc Complexes. *Chem. Rec.* **2021**, *21* (5), 1130–1143. <https://doi.org/10.1002/tcr.202100041>.

(29) Dagorne, S. Recent Developments on N-Heterocyclic Carbene Supported Zinc Complexes: Synthesis and Use in Catalysis. *Synthesis* **2018**, *50* (18), 3662–3670. <https://doi.org/10.1055/s-0037-1610088>.

(30) Grundy, M. E.; Yuan, K.; Nichol, G. S.; Ingleson, M. J. Zinc Catalysed Electrophilic C–H Borylation of Heteroarenes. *Chem. Sci.* **2021**, *12* (23), 8190–8198. <https://doi.org/10.1039/D1SC01883C>.

(31) Rit, A.; Zanardi, A.; Spaniol, T. P.; Maron, L.; Okuda, J. A Cationic Zinc Hydride Cluster Stabilized by an N-Heterocyclic Carbene: Synthesis, Reactivity, and Hydrosilylation Catalysis. *Angew. Chem. Int. Ed.* **2014**, *53* (48), 13273–13277. <https://doi.org/10.1002/anie.201408346>.

(32) Guermazi, R.; Specklin, D.; Gourlaouen, C.; de Frémont, P.; Dagorne, S. Two-Coordinate NHC-Supported ZnII Organocations: Steric and Electronic Tunability and Use in Alkyne Hydroboration Catalysis. *Eur. J. Inorg. Chem.* **2022**, *2022* (6), e202101002. <https://doi.org/10.1002/ejic.202101002>.

(33) Fliedel, C.; Vila-Vicosa, D.; Calhorda, M. J.; Dagorne, S.; Aviles, Teresa. Dinuclear Zinc-N-Heterocyclic Carbene Complexes for Either the Controlled Ring-Opening Polymerization of Lactide or the Controlled Degradation of Polylactide Under Mild Conditions. *ChemCatChem* **2014**, *6* (Copyright (C) 2020 American Chemical Society (ACS). All Rights Reserved.), 1357–1367. <https://doi.org/10.1002/cctc.201301015>.

(34) Specklin, D.; Hild, F.; Fliedel, C.; Gourlaouen, C.; Veiros, L. F.; Dagorne, S. Accessing Two-Coordinate ZnII Organocations by NHC Coordination: Synthesis, Structure, and Use as π -Lewis Acids in Alkene, Alkyne, and CO₂ Hydrosilylation. *Chem. – Eur. J.* **2017**, *23* (63), 15908–15912. <https://doi.org/10.1002/chem.201704382>.

(35) Wehmschulte, R. J.; Wojtas, L. Cationic Ethylzinc Compound: A Benzene Complex with Catalytic Activity in Hydroamination and Hydrosilylation Reactions. *Inorg. Chem.* **2011**, *50* (22), 11300–11302. <https://doi.org/10.1021/ic201921d>.

(36) Petersen, T. O.; Simone, D.; Krossing, I. From Ion-Like Ethylzinc Aluminates to [EtZn(Arene)₂]+[Al(ORF)₄]- Salts. *Chem. – Eur. J.* **2016**, *22* (44), 15847–15855. <https://doi.org/10.1002/chem.201601860>.

- (37) Friedrich, A.; Eysel, J.; Langer, J.; Harder, S. Comparison of Magnesium and Zinc in Cationic π -Arene and Halobenzene Complexes. *Organometallics* **2021**, *40* (3), 448–457. <https://doi.org/10.1021/acs.organomet.0c00786>.
- (38) Schnee, G.; Fliedel, C.; Avilés, T.; Dagorne, S. Neutral and Cationic N-Heterocyclic Carbene Zinc Adducts and the BnOH/Zn(C₆F₅)₂ Binary Mixture - Characterization and Use in the Ring-Opening Polymerization of β -Butyrolactone, Lactide, and Trimethylene Carbonate. *Eur. J. Inorg. Chem.* **2013**, *2013* (21), 3699–3709. <https://doi.org/10.1002/ejic.201300292>.
- (39) Tapu, D.; Dixon, D. A.; Roe, C. 13 C NMR Spectroscopy of “Arduengo-Type” Carbenes and Their Derivatives. *Chem. Rev.* **2009**, *109* (8), 3385–3407. <https://doi.org/10.1021/cr800521g>.
- (40) Mantina, M.; Chamberlin, A. C.; Valero, R.; Cramer, C. J.; Truhlar, D. G. Consistent van Der Waals Radii for the Whole Main Group. *J. Phys. Chem. A* **2009**, *113* (19), 5806–5812. <https://doi.org/10.1021/jp8111556>.
- (41) Gutmann, V. Solvent Effects on the Reactivities of Organometallic Compounds. *Coord. Chem. Rev.* **1976**, *18* (2), 225–255. [https://doi.org/10.1016/S0010-8545\(00\)82045-7](https://doi.org/10.1016/S0010-8545(00)82045-7).
- (42) Beckett, M. A.; Brassington, D. S.; Light, M. E.; Hursthouse, M. B. Organophosphoryl Adducts of Tris(pentafluorophenyl)borane; Crystal and Molecular Structure of B(C₆F₅)₃·Ph₃PO. *J. Chem. Soc. Dalton Trans.* **2001**, No. 11, 1768–1772. <https://doi.org/10.1039/b100981h>.
- (43) Nödling, A. R.; Müther, K.; Rohde, V. H. G.; Hilt, G.; Oestreich, M. Ferrocene-Stabilized Silicon Cations as Catalysts for Diels–Alder Reactions: Attempted Experimental Quantification of Lewis Acidity and ReactIR Kinetic Analysis. *Organometallics* **2014**, *33* (1), 302–308. <https://doi.org/10.1021/om401040y>.
- (44) Rit, A.; Spaniol, T. P.; Okuda, Jun. Dinuclear Zinc Hydride Supported by an Anionic Bis(N-Heterocyclic Carbene) Ligand. *Chem. - Asian J.* **2014**, *9* (Copyright (C) 2021 American Chemical Society (ACS). All Rights Reserved.), 612–619. <https://doi.org/10.1002/asia.201301268>.
- (45) Raz, I.; Dobrovetsky, R. Highly Chemoselective Zn⁺²-Catalyzed Hydrosilylation of Alkynes. *Chem. – Eur. J.* **2023**, *29*, e202300798. <https://doi.org/10.1002/chem.202300798>.
- (46) Check, C. T.; Henderson, W. H.; Wray, B. C.; Vanden Eynden, M. J.; Stambuli, J. P. Oxidant-Controlled Stereoselectivity in the Pd-Catalyzed Allylic Oxidation of Cis-Vinylsilanes. *J. Am. Chem. Soc.* **2011**, *133* (46), 18503–18505. <https://doi.org/10.1021/ja2089102>.
- (47) G. Dobó, D.; Sipos, D.; Sági, A.; London, G.; Juhász, K. L.; Kukovecz, Á.; Kónya, Z. Tuning the Activity and Selectivity of Phenylacetylene Hydrosilylation with Triethylsilane in the Liquid Phase over Size Controlled Pt Nanoparticles. *Catalysts* **2018**, *8* (1). <https://doi.org/10.3390/catal8010022>.
- (48) Enthaler, S.; Fu, X.-F. *Zinc Catalysis: Applications in Organic Synthesis*; Wiley, 2015.
- (49) Gérard, S.; Pressel, Y.; Riant, O. Application of N,S-Chelating Chiral Ligands and

Zinc Complexes in Catalytic Asymmetric Hydrosilylation Using Polymethylhydrosiloxane. *Tetrahedron Asymmetry* **2005**, *16* (11), 1889–1891. <https://doi.org/10.1016/j.tetasy.2005.04.025>.

(50) Enthaler, S.; Eckhardt, B.; Inoue, S.; Irran, E.; Driess, M. Facile and Efficient Reduction of Ketones in the Presence of Zinc Catalysts Modified by Phenol Ligands. *Chem. – Asian J.* **2010**, *5* (9), 2027–2035. <https://doi.org/10.1002/asia.201000317>.

(51) Kahnes, M.; Görls, H.; González, L.; Westerhausen, M. Synthesis and Catalytic Reactivity of Bis(Alkylzinc)-Hydride-Di(2-Pyridylmethyl)Amides. *Organometallics* **2010**, *29* (14), 3098–3108. <https://doi.org/10.1021/om100153z>.

(52) Marinos, N. A.; Enthaler, S.; Driess, M. High Efficiency in Catalytic Hydrosilylation of Ketones with Zinc-Based Precatalysts Featuring Hard and Soft Tridentate O,S,O-Ligands. *ChemCatChem* **2010**, *2* (7), 846–853. <https://doi.org/10.1002/cctc.201000036>.

(53) Boone, C.; Korobkov, I.; Nikonov, G. I. Unexpected Role of Zinc Hydride in Catalytic Hydrosilylation of Ketones and Nitriles. *ACS Catal.* **2013**, *3* (10), 2336–2340. <https://doi.org/10.1021/cs400581w>.

(54) Alshakova, I. D.; Nikonov, G. I. New Zinc Catalyst for Hydrosilylation of Carbonyl Compounds. *Synthesis* **2019**, *51*, 3305–3312. <https://doi.org/10.1055/s-0037-1611824>

(55) Dawkins, M. J. C.; Middleton, E.; Kefalidis, C. E.; Dange, D.; Juckel, M. M.; Maron, L.; Jones, C. Two-Coordinate Terminal Zinc Hydride Complexes: Synthesis, Structure and Preliminary Reactivity Studies. *Chem. Commun.* **2016**, *52* (69), 10490–10492. <https://doi.org/10.1039/C6CC05445E>.

(56) Adet, N.; Specklin, D.; Gourlaouen, C.; Damiens, T.; Jacques, B.; Wehmschulte, R. J.; Dagonne, S. Towards Naked Zinc(II) in the Condensed Phase: A Highly Lewis Acidic ZnII Dication Stabilized by Weakly Coordinating Carborate Anions. *Angew. Chem. - Int. Ed.* **2021**, *60* (4), 2084–2088. <https://doi.org/10.1002/anie.202012287>.

(57) Wehmschulte, R. J.; Bayliss, B.; Reed, S.; Wesenberg, C.; Morgante, P.; Peverati, R.; Neal, S.; Chouinard, C. D.; Tolosa, D.; Powell, D. R. Zinc Ammonio-Dodecaborates: Synthesis, Lewis Acid Strength, and Reactivity. *Inorg. Chem.* **2022**, *61* (18), 7032–7042. <https://doi.org/10.1021/acs.inorgchem.2c00464>.

(58) Lummis, P. A.; Momeni, M. R.; Lui, M. W.; McDonald, R.; Ferguson, M. J.; Miskolzie, M.; Brown, A.; Rivard, Eric. Accessing Zinc Monohydride Cations through Coordinative Interactions. *Angew. Chem. Int. Ed.* **2014**, *53* (Copyright (C) 2020 American Chemical Society (ACS). All Rights Reserved.), 9347–9351. <https://doi.org/10.1002/anie.201404611>.

(59) Mou, Z.; Xie, H.; Wang, M.; Liu, N.; Yao, C.; Li, L.; Liu, J.; Li, S.; Cui, D. Mononuclear Heteroscorpionate Zwitterionic Zinc Terminal Hydride: Synthesis, Reactivity, and Catalysis for Hydrosilylation of Aldehydes. *Organometallics* **2015**, *34* (16), 3944–3949. <https://doi.org/10.1021/acs.organomet.5b00413>.

(60) Li, C.; Hua, X.; Mou, Z.; Liu, X.; Cui, D. Zinc-Catalyzed Hydrosilylation Copolymerization of Aromatic Dialdehydes with Diphenylsilane. *Macromol. Rapid Commun.* **2017**, *38* (22), 1700590. <https://doi.org/10.1002/marc.201700590>.

- (61) A control NMR experiment of a 1/1 mixture of [6]⁺ and HSi(OEt)₃ (CD₂Cl₂, RT, 1 h) led to the formation of unidentified products.
- (62) Khandelwal, M.; Wehmschulte, R. J. Deoxygenative Reduction of Carbon Dioxide to Methane, Toluene, and Diphenylmethane with [Et₂Al]⁺ as Catalyst. *Angew. Chem. Int. Ed.* **2012**, *51* (29), 7323–7326. <https://doi.org/10.1002/anie.201201282>.
- (63) Adet, N.; Specklin, D.; Gourlaouen, C.; Damiens, T.; Jacques, B.; Wehmschulte, R. J.; Dagonne, S. Towards Naked Zinc(II) in the Condensed Phase: A Highly Lewis Acidic ZnII Dication Stabilized by Weakly Coordinating Carborate Anions. *Angew. Chem. Int. Ed.* **2021**, *60* (4), 2084–2088. <https://doi.org/10.1002/anie.202012287>.
- (64) Larson, G. L.; Fry, J. L. *Ionic and Organometallic-Catalyzed Organosilane Reductions*; John Wiley and Sons, Inc.: Hoboken, NJ, 2010.
- (65) Parks, D. J.; Piers, W. E. Tris(Pentafluorophenyl)Boron-Catalyzed Hydrosilation of Aromatic Aldehydes, Ketones, and Esters. *J. Am. Chem. Soc.* **1996**, *118* (39), 9440–9441. <https://doi.org/10.1021/ja961536g>.
- (66) Parks, D. J.; Blackwell, J. M.; Piers, W. E. Studies on the Mechanism of B(C₆F₅)₃-Catalyzed Hydrosilation of Carbonyl Functions. *J. Org. Chem.* **2000**, *65* (10), 3090–3098. <https://doi.org/10.1021/jo991828a>.
- (67) Oestreich, M.; Hermeke, J.; Mohr, J. A Unified Survey of Si–H and H–H Bond Activation Catalysed by Electron-Deficient Boranes. *Chem. Soc. Rev.* **2015**, *44* (8), 2202–2220. <https://doi.org/10.1039/C4CS00451E>.
- (68) Fernández-Alvarez, F. J.; Oro, L. A. Homogeneous Catalytic Reduction of CO₂ with Silicon-Hydrides, State of the Art. *ChemCatChem* **2018**, *10* (21), 4783–4796. <https://doi.org/10.1002/cctc.201800699>.
- (69) Meiries, S.; Speck, K.; Cordes, D. B.; Slawin, A. M. Z.; Nolan, S. P. [Pd(IPr*OMe)(Acac)Cl]: Tuning the N-Heterocyclic Carbene in Catalytic C–N Bond Formation. *Organometallics* **2013**, *32* (1), 330–339. <https://doi.org/10.1021/om3011867>.
- (70) Dierick, S.; Dewez, D. F.; Markó, I. E. IPr*(2-Np)—An Exceedingly Bulky N-Heterocyclic Carbene. *Organometallics* **2014**, *33* (3), 677–683. <https://doi.org/10.1021/om4008955>.
- (71) Bochmann, M. The Chemistry of Catalyst Activation: The Case of Group 4 Polymerization Catalysts †. *Organometallics* **2010**, *29* (21), 4711–4740. <https://doi.org/10.1021/om1004447>.
- (72) Azpeitia, S.; Garralda, M. A.; Huertos, M. A. Rhodium(III) Catalyzed Solvent-Free Tandem Isomerization–Hydrosilylation From Internal Alkenes to Linear Silanes. *ChemCatChem* **2017**, *9* (11), 1901–1905. <https://doi.org/10.1002/cctc.201700222>.
- (73) Rawat, S.; Bhandari, M.; Porwal, V. K.; Singh, S. Hydrosilylation of Carbonyls Catalyzed by Hydridoborenium Borate Salts: Lewis Acid Activation and Anion Mediated Pathways. *Inorg. Chem.* **2020**, *59* (10), 7195–7203. <https://doi.org/10.1021/acs.inorgchem.0c00646>.
- (74) Lipke, M. C.; Tilley, T. D. Hypercoordinate Ketone Adducts of Electrophilic η³-H₂

- SiRR' Ligands on Ruthenium as Key Intermediates for Efficient and Robust Catalytic Hydrosilylation. *J. Am. Chem. Soc.* **2014**, *136* (46), 16387–16398. <https://doi.org/10.1021/ja509073c>.
- (75) Gasperini, D.; Neale, S. E.; Mahon, M. F.; Macgregor, S. A.; Webster, R. L. Phosphirenium Ions as Masked Phosphenium Catalysts: Mechanistic Evaluation and Application in Synthesis. *ACS Catal* **2021**, *11*, 5452–5462. <https://doi.org/10.1021/acscatal.1c01133>.
- (76) Zhao, M.; Xie, W.; Cui, C. Cesium Carbonate Catalyzed Chemoselective Hydrosilylation of Aldehydes and Ketones under Solvent-Free Conditions. *Chem. - Eur. J.* **2014**, *20* (30), 9259–9262. <https://doi.org/10.1002/chem.201403497>.
- (77) Ghosh, C.; Mukhopadhyay, T. K.; Flores, M.; Groy, T. L.; Trovitch, R. J. A Pentacoordinate Mn(II) Precatalyst That Exhibits Notable Aldehyde and Ketone Hydrosilylation Turnover Frequencies. *Inorg. Chem.* **2015**, *54* (21), 10398–10406. <https://doi.org/10.1021/acs.inorgchem.5b01825>.
- (78) Khalimon, A. Y.; Simionescu, R.; Kuzmina, L. G.; Howard, J. A. K.; Nikonov, G. I. Agostic NSi□H⋯Mo Complexes: From Curiosity to Catalysis. *Angew. Chem. Int. Ed.* **2008**, *47* (40), 7701–7704. <https://doi.org/10.1002/anie.200802147>.
- (79) Noji, M.; Ohno, T.; Fuji, K.; Futaba, N.; Tajima, H.; Ishii, K. Secondary Benzylolation Using Benzyl Alcohols Catalyzed by Lanthanoid, Scandium, and Hafnium Triflate. *J. Org. Chem.* **2003**, *68* (24), 9340–9347. <https://doi.org/10.1021/jo034255h>.
- (80) Rawat, S.; Bhandari, M.; Porwal, V. K.; Singh, S. Hydrosilylation of Carbonyls Catalyzed by Hydridoborenium Borate Salts: Lewis Acid Activation and Anion Mediated Pathways. *Inorg. Chem.* **2020**, *59* (10), 7195–7203. <https://doi.org/10.1021/acs.inorgchem.0c00646>.
- (81) Petronilho, A.; Vivancos, A.; Albrecht, M. Ether Formation through Reductive Coupling of Ketones or Aldehydes Catalyzed by a Mesoionic Carbene Iridium Complex. *Catal. Sci. Technol.* **2017**, *7* (23), 5766–5774. <https://doi.org/10.1039/C7CY01832K>.
- (82) Gangwar, M. K.; Dahiya, P.; Emayavaramban, B.; Sundararaju, B. Cp*Co^{III} - Catalyzed Efficient Dehydrogenation of Secondary Alcohols. *Chem. - Asian J.* **2018**, *13* (17), 2445–2448. <https://doi.org/10.1002/asia.201800697>.
- (83) Jakobsson, K.; Chu, T.; Nikonov, G. I. Hydrosilylation of Olefins Catalyzed by Well-Defined Cationic Aluminum Complexes: Lewis Acid versus Insertion Mechanisms. *ACS Catal.* **2016**, *6* (11), 7350–7356. <https://doi.org/10.1021/acscatal.6b01694>.
- (84) Rubio, M.; Campos, J.; Carmona, E. Rhodium-Catalyzed, Efficient Deutero- and Tritiosilylation of Carbonyl Compounds from Hydrosilanes and Deuterium or Tritium. *Org. Lett.* **2011**, *13* (19), 5236–5239. <https://doi.org/10.1021/ol202117t>.
- (85) Boone, C.; Korobkov, I.; Nikonov, G. I. Unexpected Role of Zinc Hydride in Catalytic Hydrosilylation of Ketones and Nitriles. *ACS Catal.* **2013**, *3* (10), 2336–2340. <https://doi.org/10.1021/cs400581w>.
- (86) Ojima, I.; Donovan, R. J.; Clos, N. Rhodium and Cobalt Carbonyl Clusters

Rh₄(CO)₁₂, Co₂Rh₂(CO)₁₂, and Co₃Rh(CO)₁₂ as Effective Catalysts for Hydrosilylation of Isoprene, Cyclohexanone, and Cyclohexenone. *Organometallics* **1991**, *10* (8), 2606–2610. <https://doi.org/10.1021/om00054a020>.